Manuscript Details

Manuscript number	YJCRS_2019_907_R1
Title	Variation in amylose concentration to enhance wheat flour extrudability
Article type	Research Paper

Abstract

Composition and functionality of five waxy wheat (Triticum aestivum L.) genotypes were elaborately investigated and related to end-product attributes of extrudates. As such, the interaction between starch biopolymers and protein in extrusion processing could be studied. Furthermore, the effect of an increasing amylose-concentration was studied by the use of blends Waxy genotypes absorbed more water, gave rise to stiffer doughs and had higher onset and peak gelatinization temperature. In contrast, a lower pasting temperature and final viscosity and higher peak viscosity and breakdown could be observed. The volume percentage of small starch granules showed to be negatively correlated with peak temperature and positively with final viscosity and holding strength as well as with extrudate hardness. This was also positively correlated with amylose concentration. Expansion index was highest at a slightly decreased amylose concentration of 16.6%. Markedly higher moisture content for all amylose-free extrudates was attributed to a combination of increased solubility of amylopectin and reduced water evaporation at die emergence. It was hypothesized that an interplay with protein content and composition was laying at the basis of the observed differences. Moreover, the altered pasting behavior of waxy wheat may enhance the extrudability of gluten containing wheat flour.

Keywords	waxy wheat; extrusion; pasting; starch fine structure
Taxonomy	Cereal Grain Carbohydrates, Starch Function in Cereal Grains

Corresponding Author	Tom Hellemans
Order of Authors	Tom Hellemans, Humbulani Nekhudzhiga, Filip Van Bockstaele, Ya-Jane Wang, NAUSHAD EMMAMBUX, Mia Eeckhout

Suggested reviewers	Evelien Persyn, Alessandra Marti, Mario Martinez Martinez

Submission Files Included in this PDF

File Name [File Type]

Reply letter.pdf [Response to Reviewers]

Extrusion_amylose - changes.pdf [Revised Manuscript with Changes Marked]

APRM_Checklist.pdf [Revision Checklist]

Highlights.pdf [Highlights]

Graphical abstract.pdf [Graphical Abstract]

Extrusion_amylose.pdf [Manuscript File]

declaration-of-competing-interests.pdf [Conflict of Interest]

Author statement.pdf [Author Statement]

To view all the submission files, including those not included in the PDF, click on the manuscript title on your EVISE Homepage, then click 'Download zip file'.

Research Data Related to this Submission

There are no linked research data sets for this submission. The following reason is given:
Data will be made available on request

Graphical Abstract

Variation in amylose concentration to enhance wheat flour extrudability

T. Hellemans, H. Nekhudzhiga, F. Van Bockstaele, Y.J. Wang, M.N. Emmambux, M. Eeckhout

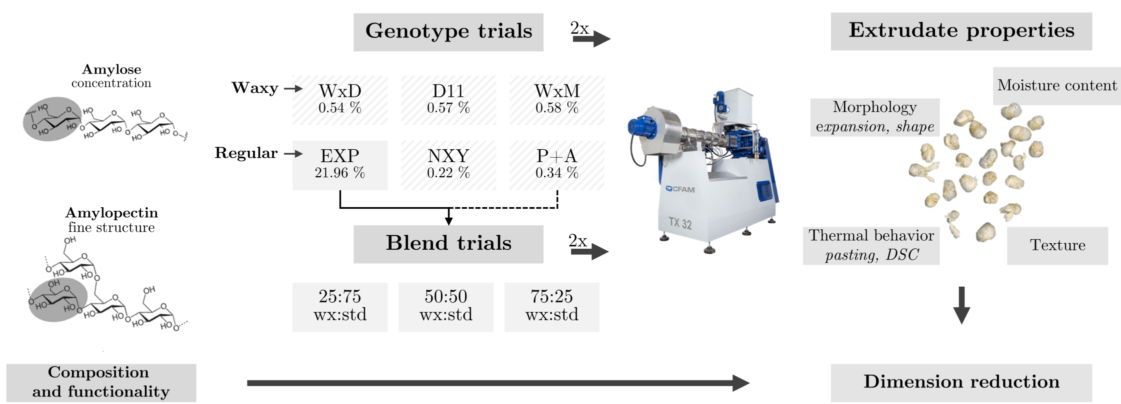

Highlights

Variation in amylose concentration to enhance wheat flour extrudability

T. Hellemans, H. Nekhudzhiga, F. Van Bockstaele, Y.J. Wang, M.N. Emmambux, M. Eeckhout

- Starch granule size distribution is related to extrudate texture.
- Amylose content affects expansion index, water absorption and texture of extrudates.
- Interaction between starch content and protein composition and quality was observed.
- Waxy genotypes are strongly varying in their protein composition and functionality.
- Maximum expansion was obtained for blends containing 25 % waxy flour.

Variation in amylose concentration to enhance wheat flour extrudability

T. Hellemans[a,*], H. Nekhudzhiga[c], F. Van Bockstaele[b], Y.J. Wang[d], M.N. Emmambux[c], M. Eeckhout[a]

[a] *Research unit on Cereal and Feed Technology, Department of Food technology, Safety and Health, Faculty of Bioscience Engineering, Ghent University, Ghent, Belgium*
[b] *Laboratory of Food technology and Engineering, Department of Food technology, Safety and Health, Faculty of Bioscience Engineering, Ghent University, Ghent, Belgium*
[c] *Department of Food and Consumer sciences Science, University of Pretoria, Pretoria 0002, South Africa*
[d] *Department of Food Science, University of Arkansas, Fayetteville, AR, USA*

Abstract

Composition and functionality of five waxy wheat (*Triticum aestivum* L.) genotypes were elaborately investigated and related to end-product attributes of extrudates. As such, the interaction between starch biopolymers and protein in extrusion processing could be studied. Furthermore, the effect of an increasing amylose-concentration was studied by the use of blends.
Waxy genotypes absorbed more water, gave rise to stiffer doughs and had higher onset and peak gelatinization temperature. In contrast, a lower pasting temperature and final viscosity and higher peak viscosity and breakdown could be observed. The volume percentage of small starch granules showed to be negatively correlated with peak temperature and positively with final viscosity and holding strength as well as with extrudate hardness. This was also positively correlated with amylose concentration. Expansion index was

*Correspondence: T.Hellemans@ugent.be; Tel.:+32-9-243-2494 (T.H.)

highest at a slightly decreased amylose concentration of 16.6 %. Markedly higher moisture content for all amylose-free extrudates was attributed to a combination of increased solubility of amylopectin and reduced water evaporation at die emergence. It was hypothesized that an interplay with protein content and composition was laying at the basis of the observed differences. Moreover, the altered pasting behavior of waxy wheat may enhance the extrudability of gluten containing wheat flour.

Keywords: waxy wheat, extrusion, pasting, starch fine structure

Declarations of interest: none

---

1. Introduction

The use of wheat (*Triticum aestivum* L.) for the production of foods for human and animal consumption is self-evident due to its global availability, a high yielding potential—with top producing countries such as Ireland (10.2 t/ha), New Zealand (9.9 t/ha), Belgium and the Netherlands (8.6 and 9.1 t/ha resp.)—and the unique viscoelastic properties (MacRitchie, 2016). Main applications of wheat are bakery products (bread, biscuits, *etc.*) that require a gluten network formation for which wheat flour has to be mixed with high amounts of water (50–65 % of the flour weight) (Barak et al., 2014; Hellemans et al., 2018). The gluten network provides a high gas retention capacity and a desirable crumb elasticity in the end-product. Extrusion processing, however, combines low water contents with a high temperature, shear rate and pressure, thereby partially abolishing the beneficial functional effects of gluten proteins. Earlier research found that both protein concentration and composition negatively affect extrudate properties such as the expansion index, water absorption and hardness (Hellemans, 2020). Pietsch et al. (2018) have shown that, on a molecular level, both the strong disulfide bond formation and hydrophobic interactions during twin-screw extrusion induce an intense polymerization of the wheat gluten. This prevents a proper expansion, thus resulting in dense and chewy instead of light and crisp extrudates. Moreover, an increased chance of blocking the extruder exists due to the high motor torques. For these reasons, mainly low quality (i.e. lower protein content) wheat cultivars are used in extrusion processing.

Nevertheless, besides protein properties, starch attributes may be employed to enhance processability and end-product quality due to the importance of both starch-starch and starch-protein interactions. For example, one of the main factors determining the extrudate properties is the melt viscosity (Robin et al., 2011) which, on its turn, has been related to the starch physicochemical properties (e.g. amylose:amylopectin-ratio, granule size distribution, presence of amylose-lipid complexes, etc.) and the starch pasting behavior (Kristiawan et al., 2018). Additionally, competition for water between protein and starch during extrusion further complexes these interactions.

In practice, the amylose content of conventional bread wheat is narrowly distributed between 25–28 %. Moreover, compared with waxy maize flour, (partial) waxy wheat flour is relatively new (Van Hung et al., 2006; Šárka and Dvoáček, 2017) and also high-amylose wheat flours (containing amylose contents up to 50–80 %) have only been commercially introduced in North America and Australia recently. Starch properties of waxy wheat flour may however provide possibilities to counteract the potential negative effects of the presence of wheat gluten proteins as it lowers the specific mechanical energy (SME) (Kowalski et al., 2015), thereby reducing the chance of ceasing the extruder. Moreover, they can also be used to obtain enhanced sensorial features or to produce high-energy foods at less demanding processing conditions due to the lower gelatinization temperature of waxy starches.

Results on the added value of waxy (wheat) flour to produce ready-to-eat (RTE) expanded snacks are however contradictory. The incorporation of waxy flour and hence, the lowering of the amylose content in the mix, had a main effect on the expansion of the extrudates. Some studies showed an increase (Kowalski et al., 2015) while in other, a decrease (Jongsutjarittam and Charoenrein, 2014; Thakur et al., 2017) in the expansion index (EI) was reported. In Jongsutjarittam and Charoenrein (2014), who compared waxy rice and rice flour based extrudates, this was attributed to the collapse during cooling. In addition, expansion was also impacted by the feed moisture content with an overall lower degree of shrinkage or collapse at high moisture contents. Despite the effects of amylose content on extrudate texture were related to differences in the EI, findings are also under discussion with both harder (Jongsutjarittam and Charoenrein, 2014) and softer (Kowalski et al., 2015) textures at lower amylose contents. As amylopectin is more sensitive to molecular degradation under extrusion conditions, waxy starches will show more short chain dextrins which lower the melt viscosity and thus, end-product properties such as the water absorption index (WAI) (Van Den Einde et al., 2004; Van den Einde et al., 2003). Under high-shear conditions (at high SMEs), molecular disruption was promoted in both regular and waxy barley flour leading to an increased WAI. This is supported by Jongsutjarittam and

Charoenrein (2014) who found that the entanglement of the linear amylose chains makes it more difficult to pull the network apart during expansion which implies the presence of intact (i.e. not (exo)degraded) polymers at increased SMEs. This network formation also resulted in a decreased EI for regular flour.

Vast amounts of research have already been performed on the relation between the amylose content and extrudate quality attributes, however, this was mainly done using rice or maize flour or starch. Kowalski et al. (2015) also stated that waxy *wheat* flours have not seen wide use in extrusion industry compared to other waxy flours (waxy maize and waxy barley). Moreover, previous studies frequently leave out intermediate amylose concentrations by studying the structure–functionality relationship using one or several pure waxy and regular cultivars. In bread, however, it has been proven that slightly reduced amylose concentrations increase end-product quality whereas 100 % waxy wheat significantly reduces structure and quality of the final product (Kowalski et al., 2015). The present work studies a range of amylose concentrations to provide additional insight in how amylose content influences end-product quality of wheat flour extrudates. Moreover, by screening multiple waxy cultivars, this study also broadens the knowledge on how genotype-dependent molecular differences may be deployed to improve waxy wheat flour applicability in extrusion processing.

2. Materials and methods

2.1. Raw materials

Five waxy wheat genotypes (table 1) were cultivated during 2017–2018 at the research farm of Ghent University and University College Ghent (Bottelare, Belgium). The field trial (Moortsele, Belgium, 50.96525 NB, 3.77977 EL) was conducted on a sandy loam soil with perennial rye grass as forefruit and was fertilized according to the advised dose rates for nitrogen (87 kg N ha^{-1}, 50 kg N ha^{-1} and 60 kg N ha^{-1} at Zadoks G.S. 22, G.S. 30 and G.S. 39, respectively). The harvested and cleaned wheat was tempered overnight to 15.5 % moisture and milled to flour using a Bühler laboratory mill. After a two week maturation period in plastic buckets at room temperature, flour samples were packed in polyethylene bags and were shipped to Pretoria (South Africa) for extrusion experiments. Regular wheat flour (so called *'Export flour'*) was obtained from Paniflower nv (Zwijnaarde, Belgium). This low-protein wheat flour (<10 %) contains no additives (e.g. vitamin C, enzymes, etc.) and is used as a reference flour throughout this research.

2.1.1. Formulation of blends

In this paper, results of two sets of extrusion trials are presented. In the blending trials (BT), the influence of the amylose content on extrusion properties and extrudate quality is studied. Therefore, waxy wheat flour (P+A) and standard bread wheat flour (EXP) were mixed in five different ratios: 100:0 (pure waxy wheat), 75:25, 50:50, 25:75, and 0:100 (pure regular wheat flour). In this way, amylose contents of approximately 0, 5.5, 11, 16.5 and 22 % were obtained. After weighing each flour in a separate bucket, a semi-industrial Hobart mixer equipped with a whisk was used to prepare homogeneous samples by mixing at low speeds for 10 minutes.

[Table 1 about here.]

2.2. Extrusion experiments

The expanded cereals were produced using a CFAM TX-32 laboratory scale co-rotating twin-screw extruder (CFAM Technologies (Pty) Ltd., Potchefstroom, South Africa). The extruder barrel consisted of five independent electrically heated and actively cooled zones. Prior to commencing the extrusion experiments, the die was preheated by the transferred heat of the fifth barrel zone. Barrel diameter D was 32.0 mm and barrel length L 500 mm (L/D-ratio = 15.65). A circular die (D = 3.0 mm) was used in combination with a single rotating knife. Results from preliminary trials were used to select suitable extruder operating conditions. Product feed rate (5 $kg\ h^{-1}$), water addition (0.28 $l\ h^{-1}$), screw speed (150 rpm), and temperature of zones 1–5 (40, 90, 100, 110, and 120 °C respectively) were kept constant during all trials. A conventional screw configuration consisting out of an initial conveying zone, two conveying and reaction zones (both ending with mixing elements), a single kneading block (for intense mixing during gelatinization) and a final conveying zone was used. All extrusion experiments were performed in duplicate in order to include processing variability in the statistical analysis.

To ensure uniform samples taking, an equilibration time of at least 4 minutes was set after changing the feed material. Both spherical extrudates and strands were produced during each trial and were allowed to cool before packing them separately in hermetically sealed HDPE containers or PP bags. For the determination of the moisture content, the spherical extrudates were immediately packed in airtight HDPE containers without prior cooling.

A part of the collected and air-cooled extrudate was milled with an analytical mill (A11, IKA, Staufen, Germany) to pass through a 500 µm sieve. The samples were kept in polyethylene bags in an airtight container and stored at 4 °C until further analysis.

2.3. Raw material composition

2.3.1. Protein content

A VarioMax C/N (Elementar Analysesystemen GmbH., Langenselbold, Germany) was used to determine the nitrogen-content of the raw materials. Four hundred milligrams (as is) of each sample was accurately (precision of 0.1 mg) weighed in a crucible and placed in the autosampler. From the obtained nitrogen-content, the protein concentration was calculated using a conversion factor of 5.7. All protein contents presented in the manuscript are expressed on dry weight by using the raw materials moisture content, determined following AACCI Method 44-15.02.

2.3.2. Starch content, composition and structure

For the measurement of the granule size distribution of the starch, the amylose content and the starch fine structure, starch extracts were prepared from the wheat flour samples according to the method descirbed in Demeke et al. (1999) with slight adaptations (Hellemans, 2020).

Starch content. Starch content of the flour samples was measured in triplicate using the enzymatic method (K-TSTA) from Megazyme (Megazyme International, Wicklow, Ireland) following AACCI method 76-13.01.

Amylose content. The molecular size distribution of the starch was characterized using high-performance size exclusion chromatography. For debranched starch, 10 mg of starch was mixed with 3.2 mL of Millipore water, boiled for 30 min, cooled down and added with 0.4 mL of acetate buffer pH 3.5. Afterward, it was incubated with 10 µL of isoamylase at 45 °C for 2 h and then boiled for 15 min, and the buffer was removed with exchange resin IONAC NM-60 H^+/OH^--form, Type I (16-50 Mesh). The HPSEC system (Waters, Milford, MA) consisted of a 515 HPLC pump with a 200-µL sample loop, an in-line degasser, a 2410 refractive index detector maintained at 40 °C, and a series Shodex OHpak columns (KB-802 and KB-804) maintained at 55 °C. The effluent is 0.1 M $NaNO_3$ and 0.02% NaN_3 at an elution rate of 0.5 mL/min. Amylopectin (AMP) and amylose (AM) content were calculated from the area of their corresponding peaks by Empower Software.

Starch fine structure. Amylopectin chain-length distribution was characterized by high-performance anion-exchange chromatography with pulsed amperometric detection (HPAEC-PAD). A 10 mg defatted starch was mixed with 3.2 mL of deionized water, heated in a boiling water bath for 30 min, cooled to room temperature, and the pH adjusted with 0.4 mL of 0.1 M acetate buffer (pH 3.5). Ten µL (10 U) of isoamylase (Pseudomonas isoamylase, Megazyme International, Wicklow, Ireland) was added and the mixture was incubated in a water bath shaker at 45 °C with stirring at 150 rpm for 2 h. The pH of the mixture was neutralized by adding 0.21 mL of 0.2 M

NaOH, heated in a boiling water bath for 15 min, and allowed to cool at room temperature for 5 min. A 1.5 mL aliquot was centrifuged at 5000 × g for 5 min in a non-stick Eppendorf tube to remove insoluble materials. A 0.6 mL supernatant was used for the HPAEC-PAD analysis using a Dionex ICS-3000 ion chromatography system (Dionex Corporation, Sunnyvale, CA) with an AS40 automated sampler, a 50-mm CarboPac PA1 guard column, and a 250-mm CarboPac PA1 analytical column. Two eluent systems (150 mM NaOH and 500 mM $NaNO_3$ in 150 mM NaOH) were used to separate the branch-chain fractions by gradient elution. Sugars with DP 1 to 7 were used to identify the chromatographic peaks. The assignment for the chromatographic peaks with DP higher than 7 was based on the assumption that each successive peak represented a saccharide that was 1 DP longer than that of the previous peak. Duplicate measurements were taken for each starch sample.

2.3.3. Starch granule size

After starch extraction, granule size distribution was determined in aqueous conditions using a Mastersizer 2000S (Malvern Panalytica, Malvern, UK) equipped with a Hydro 2000S module. Directly after initiating the measurement, starch extract (12–18 mg) was suspended in 1 mL ultrapure water using a micropipette. The suspension was added to the dispersant (water) tank until an obscuration between 11 and 16 % was obtained. During the 75 s measuring cycle, three snapshots (technical repetitions) were taken. A general purpose analysis model was used with the particle refractive index and absorption indices of 1.53 and 0.1 respectively, while the refractive index of the dispersant was 1.33. Particle size is defined in terms of 10th percentile

(D_{10}), median (D_{50}), 90th percentile (D_{90}) and the relative contribution of B-type (≤10.0 µm) and A-type (10.01–35.0 µm) granules. The proportion of granules larger than 35 µm is denoted as 'A^{+}'.

2.4. Functional properties

2.4.1. Pasting behavior

Flour (both blends and the pure genotypes) and ground extrudates pasting behavior was measured using a Physica MCR 101 Rheometer (Anton Paar, Ostfildern, Austria) equipped with a starch pasting cell with a six-blade vane. Prior to commencing the pasting cycle, flour was mixed with 15 mL distilled water whereas the ground extrudate was added during the pre-shear phase (14 % w/v, 2.1 g on dry basis). This was done to ensure that all sample was added to the water. The pre-shear—a logarithmic increase to 960 rpm while heating to 50°C during a period of 30 s—was followed by stirring at 160 rpm throughout the entire measurement. A holding phase of 1 min at 50 °C was followed by a heating phase to 95 °C at 5 °C min^{-1}. Subsequently, a holding phase at 95 °C for 5 min and cooling phase (rate equal to heating phase) was completed. The measurement was ended by a final holding phase at 50 °C for 2 min.

From the recorded curves (minimum 3 repetitions per sample), the pasting and peak temperature (T_g, P_{temp}) were determined , as well as the viscosity at the peak (PV), during the holding period (holding strength, HS) and at the end of the measurement (final viscosity, FV). The breakdown (BD) and SB_{tot} were respectively calculated as the difference between PV or FV and HS.

2.4.2. Thermal analysis

Thermal properties of both the raw material (flour) and ground extrudates was determined in duplicate using a high-pressure differential scanning calorimeter (DSC) (HP DSC827e, Mettler Toledo, Greifensee, Switzerland). Approximately 10.0 ± 0.2 mg of sample (as is) was mixed with distilled water (40 mg) in 100mg DSC-pans. Prepared samples were left at least 24 h at room temperature to equilibrate. After calibrating the equipment with Indium (Tp = 156.6 °C, 28.455 $J.g^{-1}$), scanning was performed from 30–130 °C at a rate of 3.0 °C min^{-1}. All measurements were performed at a pressure of 4 MPa using N_2. An empty pan was used as a reference.

2.4.3. Flour water absorption

A Brabender Farinograph (Brabender Technologie GmbH, Duisburg, Germany) equipped with a 50 g mixing bowl was used for determining the optimal water absorption of the flour at 500 BU following ISO 5530-1:2013. Due to the limited amount of sample, the analysis was performed once.

2.4.4. Visco-elastic dough properties

Dough visco-elastic properties were measured for the various genotypes by means of a frequency sweep using an Anton Paar MCR 102 rheometer (Anton Paar, Ostfildern, Austria). The analysis was performed at least in triplicate. Dough pieces were obtained by mixing 10.0 grams of flour with 5.9 ml distilled water using the Glutomatic apparatus (Perten Instruments, Hägersten, Sweden). After mixing for one minute, the dough piece was carefully transported to the rheometer and the measurement was started. Prior to the frequency sweep, a 20 min relaxation period was set. The measurement itself was conducted at 20 °C going from 0.1–20 Hz at 250 Pa. From the obtained storage (G') and loss (G") modulus, the phase shift angle ($\tan(\delta)$) and the complex shear modulus ($|G^*|$) was calculated. Values at 10 Hz were used for further analysis.

2.5. Extrudate properties

2.5.1. Moisture content

Moisture content was determined in threefold on the spherical extrudates using samples which were collected directly at the extruder outlet and which were stored in hermetically sealed containers. Five to thirty extrudates were counted and weighed in aluminum crucibles and were dried in two stages: at 50 °C for 24 hours and at 130 °C for another 16 hours. After cooling to room temperature, the crucibles were again weighed on an analytical balance. Moisture loss was calculated as the relative weight difference. Based on the number of extrudates, the average weight per extrudate was as well determined.

2.5.2. Expansion-index and morphology

The expansion-index (EI) of the extrudates was determined by dividing the diameter of the strands (measured in tenfold with a caliper with a 0.1 mm accuracy) by the diameter of the die outlet (3.0 mm).
Morphological parameters (area size, length-to-width ratio and circularity) of the spherical extrudates (denoted as 'kernels') were determined using the SmartGrain image analysis software, version 1.2. Scans of 50 to 100 spherical extrudates were made using an Epson Perfection 2580 flatbed scanner (Seiko Epson, Nagano, Japan) against a blue background. After equally distribut-

ing the extrudates on the scanner surface, the lid was carefully put on top of the extrudates and a scan was made at 300 DPI. Raw, non-optimized, images were stored in the .jpeg file format (maximal quality level) with a resolution of 2550 $\times$ 3510 pix. After loading the files in the software, five random background areas and extrudate areas were selected for automated color thresholding. As the software was originally developed for grain kernel analysis, the option to substract the beard of the kernels was switched off.

2.5.3. Texture

Extrudate hardness was measured using a TX.XTplus Texture Analyzer (Stable Microsystems, Godalming, United Kingdom), mounted with a 50 kg (49 N) load-cell and aluminum circular probe (P/36R, D = 36 mm). A single spherical extrudate was positioned in the center of the test platform before starting the compression test. Extrudates were compressed at 2.00 $mm\ sec^{-1}$ for a distance of 5.000 mm. Pre- and post-test speeds were set at 12.000 $mm\ sec^{-1}$ and a trigger force of 0.3 kg (2.94 N) was used to initiate data recording. Per sample, 20 replicates were performed.

Using an in-house developed R-script (version 3.4.3), the breaking strength of the spherical extrudate was defined as the maximum force of the first peak which showed a 15 % loss in measured force over a 0.16 s interval (80 data points).

2.6. Statistical analyses

For data analysis, the R software package version 3.5.1 was used. Analysis of variance (ANOVA) was used to determine whether the main effects (genotype or blending ratio) and interaction effects were significant. Principal component analysis (PCA) using the compositional, functional and end-product quality attributes was executed to obtain insight in the variability in the dataset for the different genotypes. This aided in relating the raw material properties with extrudate quality parameters. To enhance data presentation, only the two first principal components were observed. Colors of the variable arrows represent the contribution of a variable to a given principal component (in percent).

3. Results

3.1. Raw materials

Sample composition was evaluated by means of analyzing the concentration of protein and starch while from the latter, also the composition (amylose content, amylopectin fine structure), and granule size distribution was studied. Furthermore, various functional properties such as the viscoelastic behavior (by means of dynamic oscillatory rheology) and the water absorption (using the Brabender Farinograph) of the flours were determined. The average values for these analysis are shown in table 2.

The protein content of all genotypes is remarkably low for bread wheat, varying from 9.7–11.7 %dm. This may be a direct result of the limited amounts of N fertilization applied during cultivation. Due to the short growing season of spring wheat genotypes (sown in April, harvested in July), P+A has a naturally high protein content. The phase shift angles ($\tan(\delta)$) and complex shear moduli ($|G^*|$) of all waxy samples, except D11, are highly comparable under the used test conditions. This indicates that the dough has comparable visco-elastic properties at 58 % hydration. On the contrary, values for the water absorption obtained using the Brabender Farinograph ranged from 62.5 to 71.6 % for D11 and NXY respectively.

Research from Zhang et al. (2014) attributed a varying water absorption to variation in the amylose concentration and the granule size distribution. Also TSt was related to WA although it was unclear if this was directly related to the starch or if this was an indirect effect of protein dilution (Purna et al., 2011). Starch contents were not significantly differing for the waxy genotypes with exception of P+A which had a lower starch concentration (76.8 $\pm$ 2.2). The amylose content of the regular wheat flour (EXP) (21.96 $\pm$ 0.73 %) is in accordance with the range reported by Van Hung et al. (2006) and concentrations in all waxy-cultivars was below 1 %. Minor variations within this group could be observed with contents ranging from 0.22 $\pm$ 0.01 to 0.58 $\pm$ 0.04 %.

For the amylopectin (AMP) branch chain length distribution, a significantly higher average chain length (aCL) (*i.e.* DP) was seen for WxD (DP = 20.79). EXP, on the contrary, had on average shorter AMP chains (aCL = 20.03). This distinction can be related to significant differences in the distribution pattern with lesser DP 6–24 chains and more long (DP 25–65) branches for the waxy wheat flours compared to regular wheat flour (Table 2). Presence of A-type (DP = 6–12) and B_3^+ (37–65) AMP chains was negatively correlated and showed the largest variation. For the A-type chains, WxD was significantly differing from D11 and P+A which were in turn significantly lower from EXP. An opposite trend was found for the B_3^+-chains. In addition, only EXP had a significantly higher proportion of B1-type chains (DP 13–24) whereas it had a lower amount of midlong (B_2-type, DP 25–36) chains. D11 and WxD had a significant higher concentration B_2-type chains. In general, an average relative proportion of 25.59, 47.55, 17.46 and 9.41 % was found for the different chain lengths (A, B_1, B_2, B_3^+-types, respectively).

Results for the starch granule size distribution were markedly different for all genotypes except WxD and D11 who showed similar trends. Besides the relation between granule size and flour water absorption (during mixing and pasting), tan(δ) and ($|G^*|$) were found to increase for smaller granule sizes (Soh et al., 2006). However, no one-on-one correlations were observed between granule size properties and dough rheological attributes. In contrast, peak temperature in starch pasting measurements (P_{temp}) was significantly negatively correlated with the amount of B-type granules (R^2 = 0.776, p = 0.048) which might be related to their increased water absorption capacity as a result of the higher surface area to volume ratio.

[Table 2 about here.]

3.1.1. Thermal properties

In addition to the aforementioned functional properties, thermal properties of the flour (starch gelatinization and protein denaturation) was studied more in-depth by using pressurized DSC (limited amount of water) and viscosity measurements (starch pasting cell under constant stirring in excess of water). As extrusion processing partially remains a *black-box*, it is advantageous to gain a broad insight in the pasting behavior under both conditions.

DSC-profiles of the flour from the different genotypes all showed a single endotherm within a temperature range of 53.1–67.9 °C (table 2). EXP had the lowest onset (T_o) and peak (T_p) temperature (53.1 and 59.7 °C resp.)

and the second lowest endset temperature (T_e = 65.1 °C). Moreover, it was characterized by a low enthalpy (ΔH) of 2.7 $J.g^{-1}$. P+A, on the other hand, has the highest T_o (59.2 °C), T_p (63.8 °C), and T_e (67.9 °C). Both NXY and WxM, however, had higher enthalpies (6.9 $J.g^{-1}$ and 6.6 $J.g^{-1}$ resp.) compared to P+A (ΔH = 6.4 $J.g^{-1}$).

Ground extrudate powder was also subjected to DSC analysis, performed using the same methodology but did not show any significant endotherm over the entire scanning range (30–130 °C) (results not shown). This may indicate that no ungelatinized starch (i.e. intact granules) remains after extrusion cooking as was also reported by Ozcan and Jackson (2005).

Pasting profiles of the pure waxy wheat *flours* illustrate clear differences, mainly in the pasting temperature (T_g), peak viscosity (PV) and the peak temperature (P_{temp}). Genotypes WxD and D11 again show very similar trends analogous to the findings from the DSC measurements. NXY is characterized by the highest PV (3348 ± 16 mPa.s), followed by P+A (2537 ± 19 mPa.s), and WxD and D11 (≈2123 mPa.s). WxM has a significantly lower PV of 1154 ± 39 mPa.s which also results in a significantly lower holding strength (HS) and final viscosity (FV) of 128 ± 3 and 190 ± 5 mPa.s respectively. This may be an effect of the high enzyme (α-amylase) activity in the sample, resulting in a breakdown of the starch at heating (results not shown). Additionally, P+A has a higher T_g of 65.7 °C compared to all other waxy flours of which the pasting temperature is approximately 60 °C. All parameters from the pasting curves can be found in table 3.

Figure 1**B** illustrates the consequences of blending flour to obtain a specific amylose content. The two distinct peaks at approximately 6 and 10 min, which are mainly visible in the curves with blending ratios 75:25, 50:50 and 25:75, are from the waxy wheat and regular wheat respectively. At decreasing blending ratios (towards pure regular wheat flour), the PV of the first peak will decline while the second peak increases in height. Nevertheless, the total AUC for the two first peaks appears to be relatively lower for the 50:50 and 25:75 wx:std blend compared to the expected peak area. Moreover, pure flours (both pure waxy [P+A]) and regular wheat flour [EXP]) have significantly higher FVs compared to the blends (586–678 mPa.s compared to 209–289 mPa.s). Amylose is crucial during network formation upon cooling as the long molecules can form a backbone in the starch-protein network although this is depending on the molecular weight of the molecules (Singh et al., 2009a). Various researchers observed a positive correlation between amylose content and FV although the interplay with proteins, lipids and non-starch polysaccharides contributed significantly to these effects. The similar high FV for both pure waxy and pure regular wheat flour may be attributed to the amylose-to-amylopectin-ratio and the ability of amylopectin molecules to aggregate via double helix formation in the absence of distorting elements (such as amylose) (Blazek and Copeland, 2008).

[Figure 1 about here.]

[Table 3 about here.]

3.2. Extrudate characteristics

Extrudate quality was evaluated by means of their moisture content and average kernel weight, morphological attributes and texture (i.e. hardness).

Results for both the genotype trials (GT) and blending trials (BT) are shown in table 4.

Moisture content of the extrudates shows to be significantly ($p<0.001$) influenced by the genotype with D11 having the highest value of 15.7 % while P+A has the lowest value (13.9 %) for the waxy genotypes. EXP differentiates with a very low extrudate moisture content of 10.6 %. This implies an effect of the amylose content on moisture loss during expansion at die emergence. Results from the BT confirm this with extrudates made from 100:0 Wx:std having a significantly ($p<0.001$) higher MC than 50:50 blends and, subsequently, regular wheat flour (13.9 %, 12.7 % and 10.6 % respectively). Despite minor variations between average kernel weights were recorded for the various genotypes—ranging from 0.166 $g/extrudate$ for D11 to 0.221 $g/extrudate$ for NXY—no influence of amylose content ($p=0.477$) was found.

When the melt exits the die, expansion occurs as a result of the flash evaporation of water resulting in 1) a reduction of the moisture content of the extrudate, 2) a rapid decrease of the melt temperature and, consequently, a solidification of the viscous structure. By dividing the resulting diameter of the extrudate (strands) by the diameter of the die (3.0 mm), the expansion-index (EI) is obtained. Although differences in the EI were limited (ΔEI $= 0.28$), a genotypic effect ($p<0.01$) could be observed. P+A and D11 had the highest EIs (3.97 $\pm$ 0.12 and 3.94 $\pm$ 0.20 resp.) while NXY being the least expanded (3.71 $\pm$ 0.30). Additionally, amylose contents significantly affected the EI, however, the correlation was not linear. The 25:75 blend resulted in the highest value (4.16) with a decrease towards higher incorporations of waxy wheat in the blends. Regular wheat flour had the lowest EI within the BT. This might possibly be due to a collapse of the gas cells just after expansion. Based on automated image processing of scans of the spherical extrudates, the morphology could be studied. Besides area, the length-to-width ratio (LtWr) and the circularity provide additional insight in the resistance of the extrudate against collapse after expansion. All three measures are showing a significant influence of the genotype ($p<0.001$), as well as from the amylose content (i.e. blending rate) ($p<0.001$). The area size is the smallest for WxD and D11 which are both significantly differing from NXY and WxM. P+A and EXP have the highest area size. Despite the significantly lower area size for NXY-based extrudates compared to those of EXP and P+A (108 ± 18 *versus* 130 ± 26 and 126 ± 20), the LtWr and circularity of the former genotype is (almost) equal to EXP and P+A. Results from the BT clearly indicate an optimum for both LtWr and circularity at a blending ratio of 75:25 wx:std. Both lower and higher amylose contents result in increased widths, thus, decreased circularity. For the area size, no clear trend of amylose concentration was observed.

[Table 4 about here.]

Extrudate texture (i.e. crispness) is an important quality attribute for expanded *ready-to-eat* snacks as it is typical for this type of products. Despite crispness, as a sensorial parameter, can be defined in various different ways, hardness and compression distance at which the outer layer of the extrudate breaks are known to be a good indicators. Clear genotypic effects for both the hardness and compression distance are observed ($p<0.001$) with WxM and EXP having an average higher breaking strength (25.997 $\pm$ 9.575 N and 2.623 $\pm$ 0.626 N resp.) compared to all other genotypes ranging from 18.688 $\pm$ 6.043 to 21.396 $\pm$ 11.085 N). However, for the compression distance, EXP is significantly differing from all waxy genotypes. This means that, before breaking occurs, extrudates from EXP have to be compressed to a larger extent (0.76 $\pm$ 0.34 cm compared to 0.46 $\pm$ 0.24 cm), indicating that extrudates made from waxy wheat flour are more brittle. Analogues to the findings from the genotype trial, a clear effect of the amylose content on both hardness and compression distance is found ($p<0.001$). Both factors steadily increased respectively from 18.688 to 25.732 N and 0.39 to 0.77 mm upon increasing amylose concentrations (lower percentage waxy wheat flour). On the basis of the BT it was observed that extrudates produced with pure waxy wheat flour needed 7.044 N less compression force than extrudates made from regular wheat flour.

3.3. Pasting behavior

In order to obtain an insight in the water binding capacity and the presence of intact (i.e. unpasted) starch after extrusion cooking, the pasting behavior of the ground extrudates was determined. The resulting curves for both the GT and BT can be found in figure 1.

As the ground extrudate was added to the distilled water during the preshear phase, a first peak occurs at the beginning of the diagram as a result of the hydration of the starch components (amylose, amylopectin and fragmentated polysaccharides) in the extrudate. For the PV, genotypes P+A (73.2 $\pm$ 3.7 mPa.s) and WxM (75.5 $\pm$ 3.5 mPa.s) have lower values than

D11 and WxD (93.9 ± 2.4 and 98.0 ± 6.1 mPa.s resp.). Overall, viscosities remain quite low. During the heating phase, at 93.8 and 94.2 °C respectively, WxD and P+A show a small viscosity increase (first arrow around minute 11) whereas all other genotypes evolve towards a stable viscosity during the holding phase at 95 °C. These two genotypes also show a drop in their viscosity during cooling (second arrow at 23 minutes) making them return towards the expected viscosity range. FVs range from 79.0± 2.0 to 89.0 ± 5.2 mPa.s, following the same order as with the viscosity of the primary peak.

Samples from the BT only show an initial peak at the hydration of the powder (PV) as is illustrated in figure 1**B**). The effect of the amylose content in the extrudates clearly comes to expression in these pasting curves. PV values increase in an exponential way ($R^2 = 0.998$) from 74 ± 3 to 556 ± 42 mPa.s.

4. Discussion

The variation in the protein properties (both content and composition) of the wheat flour from the different genotypes may have influenced the end-product quality of the extrudates, mainly the expansion index (EI), as reported in previous research (Hellemans, 2020). In general, expansion will decrease at increasing protein concentrations with fewer but larger gas cells at high (>16 %) wheat gluten enrichment. In addition, this was found to be dependent on the composition of the (gluten) proteins as a result of their botanical origin (e.g. soy or wheat proteins), the genotype and the growth conditions. On the contrary, compared to pure wheat starch, addition of wheat gluten showed to have a stabilizing effect on gas cell formation (in terms of obtaining a more homogeneous internal structure in the extrudates) implying that an optimum for EI in function of protein content exists (Moraru and Kokini, 2003; Draganovic et al., 2013).

A positive correlation (p=0.03, R^2=0.715) between dynamic rheological parameter $|G^*|$ and farinograph water absorption could be observed. However, this result was in contrast with Van Bockstaele et al. (2008), who has reported a *negative* correlation of R^2=0.548. This difference can be explained by the use of a fixed water addition in the current study while Van Bockstaele et al. (2008) used 95 % of the optimal WA. Water is an important factor in determining the viscoelastic properties of dough as it has a dual role as inert filler and lubricant. In this study, an increase in the $|G^*|$ resembles a higher resistance to deformation as a result of different water absorptions of the flour constituents (mainly proteins and starch). Although $|G^*|$ and $\tan(\delta)$ may be valuable for predicting extrudate properties (*eg.* expansion and hardness), it can be argued that correlations between $|G^*|$ or $\tan(\delta)$ and end-product characteristics are lacking as during measurements, forces within the LVR were applied. Van Bockstaele et al. (2008), however, found a strong correlation (R^2 = 0.74) between $|G^*|$ and the bread volume. Kristiawan et al. (2016) hypothesized that these parameters could provide insight in the visco-elastic behavior of the melt (mainly the storage modulus) during extrusion which, on its turn, has been related to macroscopic expansion behavior. Relations are however not straight-forward as the latter is obtained through a complex combination of nucleation, bubble growth, coalescence, shrinkage and fixation.

Granule size distributions are strongly differing for the different genotypes which may affect starch gelatinization both in excess of water as well as during extrusion processing. As investigated by Singh et al. (2009b), starch rheology is mainly influenced by particle size whereby suspensions of large size particles tend to be more viscous compared to those of the counterpart smaller size (i.e. A and B-type granules respectively). In this study, the relative proportion of B-type granules ($\leq$10 µm) showed a significant negative correlation with the pasting temperature (T_g) ($p \leq 0.05$, R^2=0.776) whereas, for A-type granules (10–30 µm), positive correlations ($p \leq 0.05$) with the holding strength (HS) (R^2=0.815) and final viscosity (FV) (R^2=0.831) were found. The latter finding is in accordance with results from Kumar and Khatkar (2017) and can be attributed to the occupation of a relatively larger volume in the solution compared to B-granules at a similar quantity. Increased interaction between surfaces of unpasted (remnants of) starch granules after reaching the peak viscosity will thus contribute to a higher HS and FV (Hellemans et al., 2017). Also, the decrease in peak viscosity (PV) and the generally lower FV for the EXP flour compared to waxy flours was related to an increase in amylose content (Singh et al., 2009b; Kumar and Khatkar, 2017; Zi et al., 2019).

By means of principal component analysis (PCA), compositional and functional attributes of the raw materials and quality characteristics of the extrudates were related. In total, 68.9 % of the variance in the dataset could be explained by the two first PCs (figure 2). Colors of the arrows indicate the contribution of each variable going from dark blue (low) to dark red (high). The first PC (PC1, 45.3 %) is mainly correlated with starch related attributes such as TSt, granule size distribution parameters and thermal properties

(DSC and pasting) whereas the second PC (PC2, 22.1 %) resembles protein properties (farinograph water absorption, $|G^*|$ and $\tan(\delta)$).

[Figure 2 about here.]

Water absorption (WA) is negatively correlated with the expansion index ($R^2 = 0.90$) of the extrudates as well as with $|G^*|$ ($R^2 = 0.71$) and, to a lesser extend, $\tan(\delta)$ ($R^2 = 0.58$). In addition, MC of the extrudates is negatively correlated with both PV and protein content (PRO). This may be related to the increased hydrophobicity of proteins after extrusion (Wagner et al., 2011) resulting in a increased moisture loss at higher PRO. These findings also indicate the importance of PRO and composition in determining the visco-elastic behavior of the melt and, eventually, the expansion of the extrudates and the accompanying moisture loss at die emergence.

Firstly, increased molecular degradation (depolymerization and debranching) of amylopectin during extrusion of waxy wheat (Ozcan and Jackson, 2005) may result in an elevated moisture loss through evaporation as the formed gluten-starch network will have a lower water binding capacity. However, depolymerized amylopectin—occuring mainly at the $\alpha(1\rightarrow6)$-bonds—will result in an increased solubility of the obtained components (short chains), thereby promoting water binding. Moreover, as AMP contents are not significantly differing for the different genotypes, its contribution is considered to be limited. In contrast, limited network formation by the entanglement of these short amylopectin chains may decrease gel strength (Blazek and Copeland, 2008), thus promoting rupturing upon fast expansion during flash evaporation. This will also be highly dependent from the protein properties.

An increase in the protein content may improve gas cell formation by the development of a strong but flexible gluten-starch film around the gas cells (Sroan et al., 2009). Its strength is also determined by the protein composition, primarily the content of high molecular weight proteins (i.e. HMW-GS). As reported by Purna et al. (2011), gas cell formation during breadmaking also requires a good balance between elasticity and extensibility to allow the gas cells to expand and to rupture, thus enabling vapor to go out of the product. Another hypothesis is that an increased expansion promotes evaporation due to a larger contact surface. The finding is, however, contrasted by the positive correlation with both the amylose content and amylopectin average chain length. As amylopectin degradation occurs mainly at the $\alpha 1 \rightarrow 6$ bonds, it seems unlikely that water binding lies at the basis of this effect.

Both TSt and the D90 (or alternatively the proportion of A- and B-type granules) are positively correlated with extrudate hardness. Based on various research outcomes, both parameters will influence melt viscosity which was related with extrudate hardness by Zhang et al. (2016). They have stated that the thermal properties (mainly ΔH) can affect the textural characteristics of the extrudates by influencing both the specific mechanical energy and the melt viscosity. However, it has to be kept in mind that, on one hand, the melt viscosity should be low enough to promote bubble growth but, on the other hand, should be high enough to prevent bubble collapse and coalescence. Lower viscosity can lead to decreased melt strength and increase the chance of gas cell collapse (Kristiawan et al., 2016).

When studying different genotypes with an altered composition in terms of protein and starch, a broad screening of all molecular and macromolecular attributes should be attained to properly investigate the possible protein-starch interactions determining in extrudate quality. In addition, an enhanced simulation of the pasting behavior of the flour during extrusion (under high pressure, shear and temperature and at low moisture contents) or on-line viscosity measurements should be included. Inherent to the use of blends to study the effect of a single attribute is the undesirable shift in other compositional properties (in this case: protein content and composition). A possible solution would be the use of near-isogenic lines.

5. Conclusion

This study has shown that, when applying waxy wheat flour in extrusion processing, an important genetic factor should be taken into account as both protein and starch related attributes influence its processability and thus, end-product quality. Nevertheless, a minimal addition of waxy wheat flour to regular wheat flour (25:75 wx:std) enhances the expansion ratio of the extrudate while resulting in more brittle products with an overall lower hardness. Effects are however not linear with the amylose-to-amylopectin ratio and the protein composition (and their mutual interaction) being crucial factors which should be taken into consideration when assessing the relation between composition and end-product quality. Results showed that also starch granule size distribution influences the pasting and gelatinization behavior, although the primary effect may remain the starch composition as this is found to be related with the size distribution pattern. Contrastingly, no clear evidence of a relation between the average amylopectin chain length and extrudate quality was found although waxy genotypes in this study had a higher proportion short branch-chains resulting in a significantly lower average chain length.

When studying different genotypes with an altered composition in terms of protein and starch, a broad screening of all molecular and macromolecular attributes should be attained to properly investigate the possible protein-starch interactions which are determining for extrudate quality. In addition, an enhanced simulation of the pasting behavior of the flour during extrusion (under high pressure, shear and temperature and at low moisture contents) or on-line viscosity measurements should be included. An improved understanding of both the factors influencing melt viscosity as well as how this is related to end-product quality is highly recommendable. This would however require a mechanistic modeling approach.

Inherent to the use of blends to study the effect of a single attribute, is the undesirable shift obtained for other compositional properties (in this case: protein content and composition). A possible solution to overcome these secondary effects would be the use of near-isogenic lines. The added value of using lines with a similar genetic background in this type of research did already come to expression through the highly comparable results observed for WxD and D11 which are known to be closely related.

6. Acknowledgments

This research was financially supported by the FWO, Research Foundation Flanders (Grant number 1S 609 16N) and VLIR-UOS Global Minds (grant number: BE2017GMUUG0A103). Special thanks goes to the University of Pretoria (South Africa) for facilitating the extrusion experiments as well as to prof. Ravindra N. Chibbar from the University of Saskatchewan (Saskatoon, Canada) for the determination of the starch granule size distribution.

References

Barak, S., Mudgil, D., Khatkar, B.S., 2014. Influence of Gliadin and Glutenin Fractions on Rheological, Pasting, and Textural Properties of Dough. International Journal of Food Properties 17, 1428–1438. URL: `https://doi.org/10.1080/10942912.2012.717154`, doi:10.1080/10942912.2012.717154.

Blazek, J., Copeland, L., 2008. Pasting and swelling properties of wheat flour and starch in relation to amylose content. Carbohydrate Polymers 71, 380–387.

Demeke, T., Hucl, P., Abdel-Aal, E.S., Båga, M., Chibbar, R., 1999. Biochemical characterization of the wheat waxy a protein and its effect on starch properties. Cereal Chemistry 76, 694–698.

Draganovic, V., Van Der Goot, A., Boom, R., Jonkers, J., 2013. Wheat gluten in extruded fish feed: effects on morphology and on physical and functional properties. Aquaculture Nutrition 19, 845–859.

Van den Einde, R., Van der Goot, A., Boom, R., 2003. Understanding molecular weight reduction of starch during heating-shearing processes. Journal of Food Science 68, 2396–2404.

Hellemans, T., 2020. Outline of four degrees of diversification for understanding bread wheat (Triticum aestivum L.) quality. Ph.D. thesis. Ghent University.

Hellemans, T., Abera, G., De Leyn, I., Van der Meeren, P., Dewettinck, K., Eeckhout, M., De Meulenaer, B., Van Bockstaele, F., 2017. Composition, granular structure, and pasting properties of native starch extracted from plectranthus edulis (oromo dinich) tubers. Journal of Food Science 82, 2794–2804.

Hellemans, T., Landschoot, S., Dewitte, K., Van Bockstaele, F., Vermeir, P., Eeckhout, M., Haesaert, G., 2018. Impact of crop husbandry practices and environmental conditions on wheat composition and quality: a review. Journal of Agricultural and Food Chemistry 66, 2491–2509.

Jongsutjarittam, O., Charoenrein, S., 2014. The effect of moisture content on physicochemical properties of extruded waxy and non-waxy rice flour. Carbohydrate Polymers 114, 133–140.

Kowalski, R.J., Morris, C.F., Ganjyal, G.M., 2015. Waxy soft white wheat: extrusion characteristics and thermal and rheological properties. Cereal Chemistry 92, 145–153.

Kristiawan, M., Chaunier, L., Della Valle, G., Ndiaye, A., Vergnes, B., 2016. Modeling of starchy melts expansion by extrusion. Trends in Food Science & Technology 48, 13–26.

Kristiawan, M., Micard, V., Maladira, P., Alchamieh, C., Maigret, J.E., Réguerre, A.L., Emin, M.A., Della Valle, G., 2018. Multi-scale structural changes of starch and proteins during pea flour extrusion. Food Research International 108, 203–215.

Kumar, R., Khatkar, B., 2017. Thermal, pasting and morphological properties of starch granules of wheat (triticum aestivum l.) varieties. Journal of Food Science and Technology 54, 2403–2410.

MacRitchie, F., 2016. Seventy years of research into breadmaking quality. Journal of Cereal Science 70, 123–131.

Moraru, C., Kokini, J., 2003. Nucleation and expansion during extrusion and microwave heating of cereal foods. Comprehensive Reviews in Food Science and Food Safety 2, 147–165.

Ozcan, S., Jackson, D.S., 2005. Functionality behavior of raw and extruded corn starch mixtures. Cereal Chemistry 82, 223–227.

Pietsch, V.L., Karbstein, H.P., Emin, M.A., 2018. Kinetics of wheat gluten polymerization at extrusion-like conditions relevant for the production of meat analog products. Food Hydrocolloids 85, 102–109.

Purna, S.K.G., Miller, R.A., Seib, P.A., Graybosch, R.A., Shi, Y.C., 2011. Volume, texture, and molecular mechanism behind the collapse of bread made with different levels of hard waxy wheat flours. Journal of Cereal Science 54, 37–43.

Robin, F., Bovet, N., Pineau, N., Schuchmann, H.P., Palzer, S., 2011. Online shear viscosity measurement of starchy melts enriched in wheat bran. Journal of Food Science 76, E405–E412.

Šárka, E., Dvoáček, V., 2017. New processing and applications of waxy starch (a review). Journal of Food Engineering 206, 77–87.

Singh, N., Singh, S., Isono, N., Noda, T., Singh, A.M., 2009a. Diversity in amylopectin structure, thermal and pasting properties of starches from wheat varieties/lines. International Journal of Biological Macromolecules 45, 298–304.

Singh, S., Singh, N., Isono, N., Noda, T., 2009b. Relationship of granule size distribution and amylopectin structure with pasting, thermal, and retrogradation properties in wheat starch. Journal of Agricultural and Food Chemistry 58, 1180–1188.

Soh, H., Sissons, M., Turner, M., 2006. Effect of starch granule size distribution and elevated amylose content on durum dough rheology and spaghetti cooking quality. Cereal Chemistry 83, 513–519.

Sroan, B.S., Bean, S.R., MacRitchie, F., 2009. Mechanism of gas cell stabilization in bread making. i. the primary gluten–starch matrix. Journal of Cereal Science 49, 32–40.

Thakur, S., Singh, N., Kaur, A., Singh, B., 2017. Effect of extrusion on physicochemical properties, digestibility, and phenolic profiles of grit fractions obtained from dry milling of normal and waxy corn. Journal of Food Science 82, 1101–1109.

Van Bockstaele, F., De Leyn, I., Eeckhout, M., Dewettinck, K., 2008. Rheological properties of wheat flour dough and their relationship with bread volume. ii. dynamic oscillation measurements. Cereal Chemistry 85, 762–768.

Van Den Einde, R., Akkermans, C., Van Der Goot, A., Boom, R., 2004. Molecular breakdown of corn starch by thermal and mechanical effects. Carbohydrate Polymers 56, 415–422.

Van Hung, P., Maeda, T., Morita, N., 2006. Waxy and high-amylose wheat starches and flours, characteristics, functionality and application. Trends in Food Science & Technology 17, 448–456.

Wagner, M., Morel, M.H., Bonicel, J., Cuq, B., 2011. Mechanisms of heat-mediated aggregation of wheat gluten protein upon pasta processing. Journal of Agricultural and Food Chemistry 59, 3146–3154.

Zhang, H., Zhang, W., Xu, C., Zhou, X., 2014. Studies on the rheological and gelatinization characteristics of waxy wheat flour. International Journal of Biological Macromolecules 64, 123–129.

Zhang, W., Li, S., Zhang, B., Drago, S.R., Zhang, J., 2016. Relationships between the gelatinization of starches and the textural properties of extruded texturized soybean protein-starch systems. Journal of Food Engineering 174, 29–36.

Zi, Y., Shen, H., Dai, S., Ma, X., Ju, W., Wang, C., Guo, J., Liu, A., Cheng, D., Li, H., et al., 2019. Comparison of starch physicochemical properties of wheat cultivars differing in bread-and noodle-making quality. Food Hydrocolloids 93, 78–86.

List of Figures

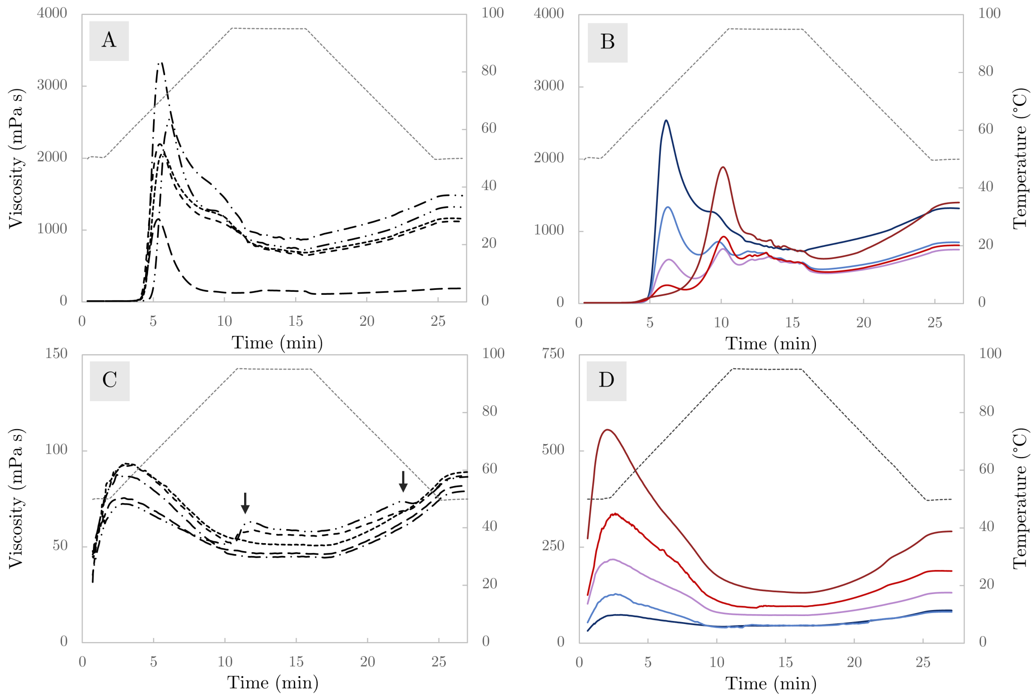

Figure 1: Pasting profiles of pure waxy wheat flours (**A**) and extrudates (**C**) (WxD - - , D11 ---, WxM ┈┈, NXY -·-, P+A -··-) and blends of waxy and regular wheat flour (**B**) and the resulting extrudates (**D**) (100:0 wx:std —, 75:25 —, 50:50 —, 25:75 —, 0:100 —, temperature ┈┈).

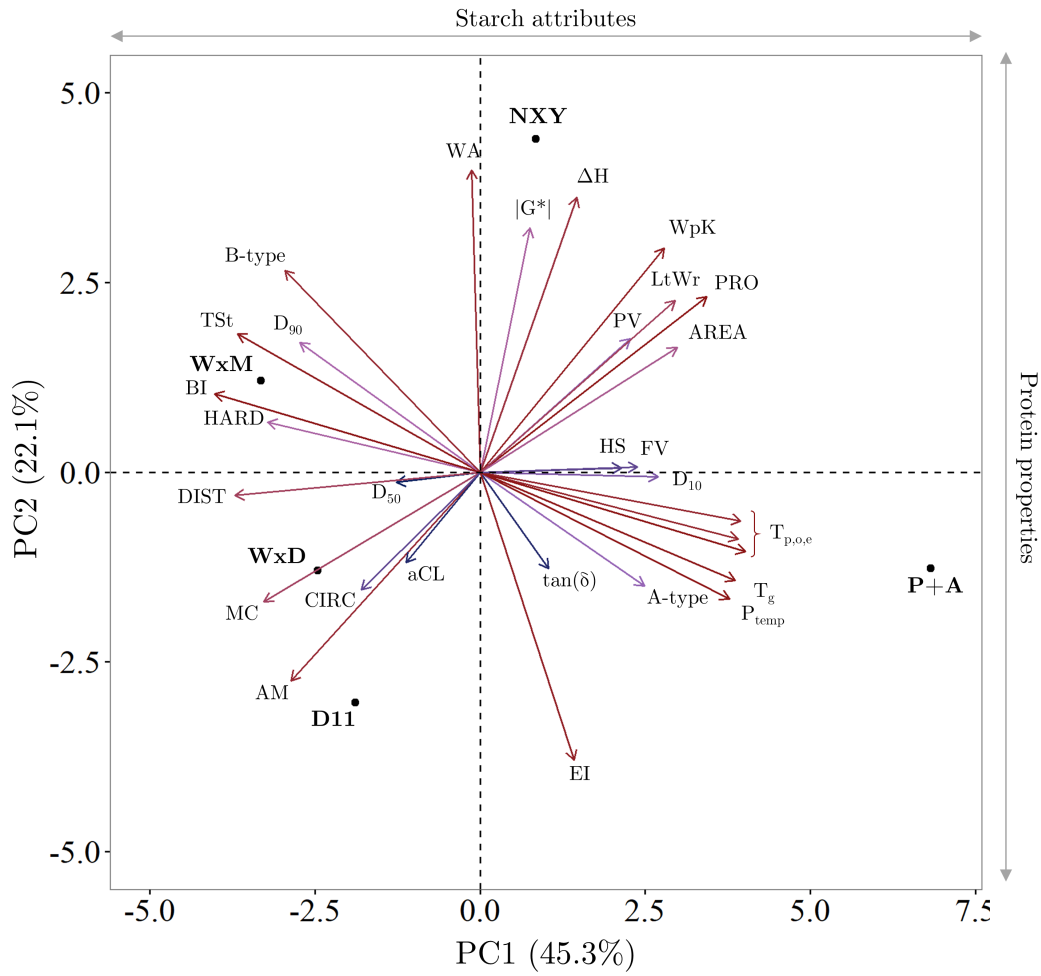

Figure 2: Biplot from the two first principal components (PC), together explaining 67.4 % of the variance in the dataset, based on compositional, functional and end-product quality attributes of the samples used in the genotype trial. The color of the arrows indicate the contribution—from dark blue (low contribution) to dark red (high contribution)—of each variable to the PCA.

List of Tables

Table 1: Overview of the wheat genotypes used in the experiments

Genotype	Owner	Origin	Wheat type	Code
WaxyDie	Dieckmann Seeds	Research farm	Winter wheat	WxD
1154.06	Dieckmann Seeds	Research farm	Winter wheat	D11
Waxymum	Limagrain Céréales Ingrédients SAS	Research farm	Winter wheat	WxM
NX12Y48222	USDA ARS (Bob Graybosch)	Research farm	Winter wheat	NXY
Penawawa+Alpowa	Washington State University (Craig Morris)	Research farm	Spring wheat (blend)	P+A
Export flour	Brabomills nv. (Paniflower)	Commercial flour	Unknown (blend)	EXP

Table 2: Composition and functionality of the raw materials (waxy flours and reference flour).

		WaxyDie	**1154.06**	**Waxymum**	**NX12Y48222**	**Penawawa+Alpowa**	**Waxy flours**[2]	**Export flour**
Composition	*PROC* (%dm)	9.7 ± 0.0	10.0 ± 0.0	10.2 ± 0.0	11.7 ± 0.0	11.7 ± 0.0	10.7 ± 1.0	9.7 ± 0.01
	TSt (% dm)	80.5 ± 4.2	80.8 ± 0.8	81.6 ± 2.6	81.6 ± 1.8	76.8 ± 2.2	80.3 ± 2.0	na
	AM (%)	0.54 ± 0.04	0.57 ± 0.12	0.58 ± 0.08	0.22 ± 0.01	0.34 ± 0.03	0.45 ± 0.16	21.96 ± 0.73
	AMP A (%)	24.60 ± 0.06	25.19 ± 0.19	25.77 ± 0.18	25.71 ± 0.09	25.53 ± 0.24	25.36 ± 0.46	26.73 ± 0.17
	AMP B_1 (%)	47.36 ± 0.08	47.56 ± 0.17	47.18 ± 0.25	47.48 ± 0.06	47.41 ± 0.11	47.40 ± 0.20	48.28 ± 0.08
	AMP B_2 (%)	18.37 ± 0.00	17.99 ± 0.06	17.33 ± 0.13	17.27 ± 0.20	17.41 ± 0.25	17.67 ± 0.46	16.39 ± 0.11
	AMP B_3^+ (%)	9.68 ± 0.02	9.26 ± 0.04	9.71 ± 0.06	9.53 ± 0.06	9.65 ± 0.10	9.57 ± 0.18	8.60 ± 0.02
	AMP aCL (%)	20.79 ± 0.01	20.53 ± 0.01	20.58 ± 0.02	20.53 ± 0.02	20.58 ± 0.08	20.60 ± 0.11	20.03 ± 0.01
	D_{10} (µm)	9.2 ± 0.1	1.2 ± 0.3	4.7 ± 0.1	5.4 ± 0.1	11.4 ± 0.0	8.2 ± 2.9	na
	D_{50} (µm)	20.8 ± 0.1	22.6 ± 0.3	20.5 ± 0.1	21.9 ± 0.1	20.3 ± 0.0	21.2 ± 1.0	na
	D_{90} (µm)	39.6 ± 0.2	46.6 ± 1.1	45.5 ± 0.2	47.0 ± 0.1	35.7 ± 0.0	42.9 ± 5.0	na
	B-type (%)	11.8 ± 0.2	9.7 ± 0.5	19.7 ± 0.3	15.3 ± 0.2	5.5 ± 0.0	12.4 ± 5.4	na
	A-type (%)	72.8 ± 0.1	68.5 ± 0.4	60.4 ± 0.1	63.0 ± 0.2	83.5 ± 0.0	69.7 ± 9.1	na
	A^+ (%)	15.4 ± 0.1	21.8 ± 0.9	19.8 ± 0.6	21.6 ± 0.2	11.0 ± 0.2	17.9 ± 4.66	na
Functional proper-ties	*Water absorption*[1] (%)	65.9	62.5	65.7	71.6	63.9	65.9 ± 3.5	60.1
	tan(δ) (rad)	0.30 ± 0.01	0.33 ± 0.01	0.33 ± 0.00	0.31 ± 0.01	0.32 ± 0.01	0.32 ± 0.01	0.36 ± 0.01
	$\|G^*\|$ (MPa)	264 ± 29	164 ± 10	266 ± 62	288 ± 66	255 ± 42	247 ± 48	150 ± 9
	T_o (°C)	56.0	56.9	56.6	56.7	59.2	57.1 ± 1.2	53.1
	T_p (°C)	60.0	61.5	60.7	61.4	63.8	61.5 ± 1.4	59.7
	T_e (°C)	65.0	65.7	65.1	65.5	67.9	65.8 ± 1.2	65.1
	ΔH (Jg^{-1})	5.4	5.4	6.6	6.9	6.4	6.1 ± 0.7	5.4

tan(δ), phase shift angle; $|G^*|$, complex shear modulus; TSt, total starch; AM, amylose content; aCL, average branch-chain length of amylopectin; D_i, i^{th} percentile of the granule size distribution; $T_{o,p,e}$, onset, peak and endset temperature; ΔH, enthalpy

[1] Water absorption at 500 BU as determined by Brabender Farinograph

[2] Mean ± stdev for waxy cultivars

Analysis of variance (ANOVA) was not performed as mean and standard deviation are based on three values (n=3)

Table 3: Overview of the results from the starch pasting behavior of flour from pure genotypes and blends (14 %db) using a Physica MCR 101 rheometer (Anton Paar, Ostfildern, Austria)

Genotype	$\mathbf{T}_g$ (°C)	**PV** (mPa.s)	$\mathbf{P}_{temp}$ (°C)	**HS** (mPa.s)	**BD** (mPa.s)	**FV** (mPa.s)	$\mathbf{SB}_{tot}$ (mPa.s)
WaxyDie	59.3 ± 0.0	2189 ± 52	69.8 ± 0.6	664 ± 4	1525 ± 48	1120 ± 4	456 ± 8
1154.06	60.2 ± 0.0	2056 ± 10	71.2 ± 0.0	692 ± 16	1364 ± 6	1158 ± 4	466 ± 12
Waxymum	59.3 ± 0.0	1154 ± 39	69.4 ± 0.0	128 ± 3	1026 ± 36	190 ± 5	62 ± 1
NX12Y48222	59.3 ± 0.0	3348 ± 16	70.3 ± 0.0	860 ± 3	2488 ± 19	1480 ± 11	620 ± 8
mean	59.5	2187	70.2	586	1601	987	401
stdev	0.5	900	0.8	317	627	555	238
100:0 wx:std	65.7 ± 0.0	2537 ± 19	73.1 ± 0.0	732 ± 4	1804 ± 22	1318 ± 4	586 ± 8
75:25 wx:std	65.7 ± 0.0	1335 ± 10	74.0 ± 0.0	559 ± 3	777 ± 13	848 ± 7	289 ± 8
50:50 wx:std	65.7 ± 0.0	610 ± 31	74.0 ± 0.0	537 ± 27	219 ± 13	746 ± 7	209 ± 34
25:75 wx:std	65.7 ± 0.0	259 ± 1	79.0 ± 7.2	565 ± 0	364 ± 24	808 ± 64	243 ± 64
0:100 wx:std	80.1 ± 0.5	1891 ± 78	93.0 ± 0.0	722 ± 14	1169 ± 65	1400 ± 131	678 ± 120

T_g, pasting temperature; PV, peak viscosity; P_{temp}, peak temperature; HS, holding strength; BD, breakdown (PV-HS); FV, final viscosity; SB_{tot}, total setback (FV-HS)

PV is defined as the y-value of the peak during the first heating phase or, if no peak is present, the first peak during the subsequent holding phase.

BD is calculated as the difference between the y-value (viscosity) of the highest peak and the HS.

analysis of variance was not performed as mean and standard deviation are based on three values (n=3)

Table 4: Quality attributes of extrudates from genotype trials and blend trials

Genotype	**MC** (%)	**WpK** (g)	**EI**	**Area** (mm^2)	**LtWr**	**Circularity**	**Hardness** (N)	**Distance** (mm)	**BI**[1] (%)
WaxyDie	14.9 ± 0.6^{ab}	0.188 ± 0.008^{c}	3.85 ± 0.24^{ab}	94 ± 15^{c}	1.20 ± 0.13^{d}	0.814 ± 0.050^{a}	21.396 ± 11.085^{ab}	0.51 ± 0.25^{b}	3.8
1154.06	15.7 ± 0.1^{a}	0.166 ± 0.014^{d}	3.94 ± 0.22^{a}	84 ± 17^{d}	1.26 ± 0.19^{c}	0.789 ± 0.085^{ab}	21.141 ± 9.879^{ab}	0.48 ± 0.25^{b}	3.9
Waxymum	14.8 ± 0.4^{bc}	0.197 ± 0.005^{bc}	3.84 ± 0.17^{c}	112 ± 20^{b}	1.31 ± 0.13^{b}	0.804 ± 0.048^{b}	25.997 ± 11.085^{a}	0.46 ± 0.28^{b}	4.3
NX12Y48222	14.5 ± 0.6^{bc}	0.220 ± 0.004^{a}	3.71 ± 0.30^{b}	108 ± 19^{b}	1.36 ± 0.15^{a}	0.781 ± 0.065^{c}	20.297 ± 10.379^{ab}	0.46 ± 0.23^{b}	3.8
mean	14.9	0.193	3.84	99	1.28	0.797	23.052	0.455	3.9
stdev	0.5	0.022	0.11	13	0.07	0.015	1.798	0.034	0.2
100:0 wx:std	13.9 ± 0.4^{a}	0.218 ± 0.010^{a}	3.97 ± 0.12^{bc}	126 ± 205^{bc}	1.37 ± 0.14^{a}	0.793 ± 0.052^{b}	18.688 ± 6.043^{c}	0.39 ± 0.19^{c}	2.8
75:25 wx:std	13.7 ± 0.3^{a}	0.213 ± 0.019^{a}	3.92 ± 0.24^{bc}	116 ± 205^{bc}	1.25 ± 0.20^{c}	0.790 ± 0.086^{a}	19.846 ± 7.956^{bc}	0.40 ± 0.22^{c}	3.1
50:50 wx:std	12.7 ± 0.5^{b}	0.212 ± 0.008^{a}	4.09 ± 0.18^{ab}	136 ± 205^{ab}	1.27 ± 0.14^{b}	0.797 ± 0.063^{ab}	20.120 ± 6.690^{bc}	0.51 ± 0.26^{bc}	4.1
25:75 wx:std	12.3 ± 0.7^{b}	0.221 ± 0.004^{a}	4.16 ± 0.18^{a}	131 ± 195^{a}	1.31 ± 0.17^{b}	0.778 ± 0.090^{ab}	24.142 ± 8.907^{ab}	0.58 ± 0.24^{b}	4.9
0:100 wx:std	10.6 ± 0.0^{c}	0.209 ± 0.008^{a}	3.85 ± 0.24^{c}	130 ± 275^{c}	1.39 ± 0.15^{a}	0.756 ± 0.091^{c}	25.732 ± 6.141^{a}	0.77 ± 0.33^{a}	6.6

MC, moisture content (n=3); EI, expansion-index (n=10); WpK, weight per kernel (n=3); LtWr, length-to-width-ratio (n⩾44); BI, breaking-index
Means with the same superscript in the same column are significantly different ($p<0.05$, Tukey's HSD)
[1]Breaking index is defined as the relative compression depth before breaking of the extrudate occurs

SUBMISSION CHECKLIST

To be completed and uploaded with the manuscript at submission.
Incomplete submissions will not be put into the peer-review process until requirements are met. Incomplete submissions will be removed from the system after 90 days.

A more complete description of each item that must be checked, including ethical considerations, is provided under the appropriate heading in the Information for Authors document available at www.archives-pmr.org.
All elements of the manuscript are printed in English and double-spaced with 1-inch margins at top, bottom, and sides. Right margins are unjustified.
Separate documents are submitted in the following order: (1) cover letter; (2) title page, including acknowledgments and explanation of any conflicts of interest; (3) main text file (manuscript without author identifiers) including a structured or standard abstract, keywords, list of abbreviations, body of the text, references, suppliers' list, figure legends; (4) figures; (5) tables; (6) appropriate completed reporting guideline (e.g. CONSORT, PRISMA, etc.) (7) appendices; (8) supplementary files; (9) author checklist; (10) disclosure forms (ICMJE Form for Disclosure of Potential Conflicts of Interest.

Cover Letter

The cover letter should include essential information, including who the corresponding author will be and a statement signed by the corresponding author that written permission has been obtained from all persons named in the Acknowledgments and patient consent forms have been collected, if needed.

Title Page

These elements are in the following sequence and are typed double-spaced.

☐Running head of no more than 40 character spaces.

☐Title.

☐Author(s) full name(s) written as First Name then Last Name, and highest academic degree(s).

☐The name(s) of the institution(s), section(s), division(s), and department(s) where the study was performed and the institutional affiliation(s) of the author(s) at the time of the study. An asterisk after an author's name and a footnote may indicate a change in affiliation.

☐Acknowledgment of any presentation of this material, to whom, when, and where.

☐Acknowledgment of financial support, including grant numbers.

☐Explanation of any conflicts of interest.

☐Name, address, business telephone number, and e-mail address of corresponding author and the author from whom reprints can be obtained.

☐If reprints are not available, this is stated on the title page.

☐Clinical trial registration number, if applicable.

Manuscript Body

☐Archives uses a double-blind peer-review process. The blinded submission should be submitted in a word document and should begin with a title followed by the abstract and then the text.

☐This document is consecutively line numbered.

☐If this is a randomized controlled trial, provide the CONSORT flow diagram (http://www.consort-statement.org/Downloads/flowchart.doc).

☐Statement is included in the body of the manuscript that human experimentation has been approved by the local institutional review board or conforms to Helsinki Declaration, as stated in the section Manuscript Preparation, Methods.

☐Guidelines for the care/use of nonhuman animals or other species, approved by the institution, have been followed as indicated in the Methods. The species is named in the title, abstract, and Methods section.

☐It is recommended that a professional editor or a colleague fluent in English edit the manuscript before submission for authors whose first language is not English.

☐The body of the manuscript includes the Introduction (no heading needed), Methods, Results, Discussion, Study Limitations (subheading), and Conclusions headings. Longer articles may need other subsection headings to clarify their content, especially the Results and Discussion sections. Other types of articles such as Commentaries and Special Communications do not require this format.

☐Footnotes other than for references are not allowed in the manuscript body.

Abstract

☐For Original Research Articles, Brief Reports, and Review Articles, a structured abstract of 275 words or fewer with Key Words is included before the body of the manuscript and is headed by the title. Note that original research and reviews have different formats for their abstracts.

☐ For other manuscripts (e.g., Commentaries, Editorials and Special Communications), include a conventional, unstructured abstract of no more than 250 words with Key Words before the body of the manuscript and headed by the title.

Abbreviations

☐Authors should include a list of abbreviations in their manuscript file following the abstract (just above introduction). Archives uses only standard abbreviations with Davis's and Dorland's as our guides. Abbreviations that are used ONLY in tables, appendices, or figures are not included in the list and should be defined in the relevant table, appendix, or figure note; however, abbreviations that are in the list need not be re-defined in a table footnote or legend. All abbreviations must be defined on first mention in the body of the manuscript. The abbreviations SD (standard deviation) and SE (standard error) require no definition in Archives.

References

☐All references have been checked for accuracy and completeness.

☐All references are numbered consecutively in the order they are cited in the text; all listed references have been cited in the text.

☐For any reference cited as "in press," a copy of the article is included.

☐Personal communications and unpublished observations are not used as numbered references but are mentioned in the text with the written approval of the person being quoted. Author must include a copy of the approval.

☐Suppliers are not listed in the reference list or included in the reference numbering (see below).
Suppliers
☐Provide a list (after the Reference section) including all manufacturers and other nondrug products used directly in the study. They should be in an alphabetized, superscripted list (i.e., a, b, c…).
☐Provide names for each Supplier.
☐Equipment and/or materials are identified in text, tables, and legends by superscript lower case letters, corresponding to the list of suppliers.
☐Suppliers are listed consecutively in the order they are cited in the text. **Figure Legends**
☐A list of figure legends should be provided after the reference list and suppliers' list, listing each figure in order by number.
☐Legends/captions should not be embedded in the figure files themselves.
Figures
☐Each is numbered with an Arabic numeral and cited in numeric sequence in the text.
☐Each figure is provided in a separate document
☐Photographs of recognizable persons require a signed release from the patient or legal guardian authorizing publication. Masking eyes to hide identity is not sufficient. (Author should be able to provide signed release forms when requested.)
☐If a CONSORT diagram is included, it should be assigned a figure number and be included with the list of figure legends.
☐Figures should be submitted in PDF, JPG, EPS, or TIFF format.
Tables
☐Each table is provided in a separate document, headed by a title, and numbered in Arabic numerals.
☐Tables are cited in numeric sequence in the text.
☐Tables should be submitted in Word or as a PDF. Please do not import tables into a Word document.
☐Reporting Guidelines

To ensure a high and consistent quality of research reporting, original research articles must contain sufficient information to allow readers to understand how a study was designed and conducted. For review articles, systematic or narrative, readers should be informed of the rationale and details behind the literature search strategy. **To achieve this goal, *Archives*, requires that authors upload a completed checklist for the appropriate reporting guideline during original submission**. The Archives specifically **requests** that the following Reporting Guidelines are used when appropriate and **strongly encourages** authors to use ***any*** of the Guidelines listed in the Equator Network **(www.equator-network.org):**

- Randomized Controlled Trials – CONSORT - Consolidated Standards of Reporting Trials
- Observational Studies – STROBE – Strengthening the Reporting of Observational studies in Epidemiology
- Systematic Review of Controlled Trials – PRISMA – Preferred Reporting Items for Systematic Reviews and Meta-Analyses

▯ Study of Diagnostic accuracy/assessment scale – STARD – Standards for the Reporting of Diagnostic Accuracy Studies
▯ Case Reports – CARE – for case reports

Highlights and Graphical Abstracts (optional)

☐Highlights are a short collection of bullet points that convey the core findings and provide readers with a quick textual overview of the article. Highlights should be submitted as a separate MS Word file in EES by selecting "Highlights" from the drop-down list when uploading files. Include 3 to 5 highlights. There should be a maximum of 85 characters, including spaces, per highlight. Only the core results of the paper should be covered. See http://www.elsevier.com/journal-authors/highlights

☐For Graphical Abstracts, authors must provide an image that clearly represents the work described in the paper. A key figure from the original paper, summarizing the content can also be submitted as a graphical abstract. Graphical Abstracts should be submitted as a separate file in EES by selecting "Graphical Abstracts" from the drop-down list when uploading files. Preferred file types are TIFF, EPS, PDF or MS Office files. See http://www.elsevier.com/journal- authors/graphical-abstract

Similar Publication

☐Upload with the manuscript files a reprint of each article and/or abstract the author and/or coauthors have previously published or is "in press," and each manuscript the author and/or coauthors have submitted for possible publication or have in manuscript form dealing with the same patients, animals, laboratory experiment, or data, in part or in full, as those reported in the submitted manuscript. Further explanation of the circumstances should be included in the cover letter, including similarities and differences.

Disclosure Forms

The ICMJE form only needs to be submitted for the corresponding author at the time of the original submission. But ICMJE forms will be needed from all authors should the manuscript move into the revision phase.

DEVICE STATEMENT

Please check off ONE statement below that pertains to your submitted work.

- The manuscript submitted does not contain information about medical device(s).
- The device(s) is/are FDA approved for the indicated usage in the United States.
- The legal/regulatory status of the device(s) that is/are the subject of this manuscript is/are not applicable in the country where the author(s) resides.
- The device(s) that is/are the subject of this manuscript has/have been cleared through the Premarket Notification (510(k)) process/approved through a Premarket Approval application for the indications studied.
- The device(s) that is/are the subject of this manuscript has/have been cleared through the Premarket Notification (510(k)) process/approved through a Premarket Approval application for [state the specific indication on a separate page and attach], but not for the indications that were reported.
- The device(s) that is/are the subject of this manuscript is/are being evaluated as part of an ongoing FDA-approved investigational protocol (DE) for [state the intended use on a separate

page and attach].

- The device(s) that is/are the subject of this manuscript is/are exempt from FDA regulations because [state reason on a separate page and attach].

- The device(s) that is/are the subject of this manuscript is/are not FDA-approved and is/are not commercially available in the United States.

- The device(s) that is/are the subject of this manuscript is/are not intended for human use.

- The legal/regulatory status of the device(s) that is/are subject of this manuscript is/are not known by the author(s).

Permissions

☐Signed, written permission from both the copyright holder and the original author for the use of tables, figures, or quotations previously published and their complete references is on file with the author and can be submitted to the editorial office upon request.

☐Signed, written permission for the use of quotations of personal communications and unpublished data has been obtained from the person(s) being quoted and is included with the submission.

☐Informed consent and releases to publish photographs of recognizable persons should be on file with the author and submitted to the editorial office upon request. Submit with the manuscript written permission to use nonoriginal material (quotations exceeding 100 words, any table or illustration) from both author and publisher of the original. No article will be accepted as a submission to Archives without all required permissions. Credit the source in a text or table note or in a legend.

Resubmissions

☐When resubmitting a manuscript for further consideration, provide an itemized accounting of how the manuscript was changed in response to the original set of evaluations. Also, a highlighted or marked-up (Track Changes) copy should be submitted showing all of the changes made throughout the manuscript.

☐Both a clean and marked-up copy of the manuscript files that were revised are required at submission.

I have reviewed this Checklist and have complied with its requirements.

Type in name above Type in date above

Tom Hellemans; 29/04/2020

Highlights

Variation in amylose concentration to enhance wheat flour extrudability

T. Hellemans, H. Nekhudzhiga, F. Van Bockstaele, Y.J. Wang, M.N. Emmambux, M. Eeckhout

- Starch granule size distribution is related to extrudate texture.
- Amylose content affects expansion index, water absorption and texture of extrudates.
- Interaction between starch content and protein composition and quality was observed.
- Waxy genotypes are strongly varying in their protein composition and functionality.
- Maximum expansion was obtained for blends containing 25 % waxy flour.

Graphical Abstract

Variation in amylose concentration to enhance wheat flour extrudability

T. Hellemans, H. Nekhudzhiga, F. Van Bockstaele, Y.J. Wang, M.N. Emmambux, M. Eeckhout

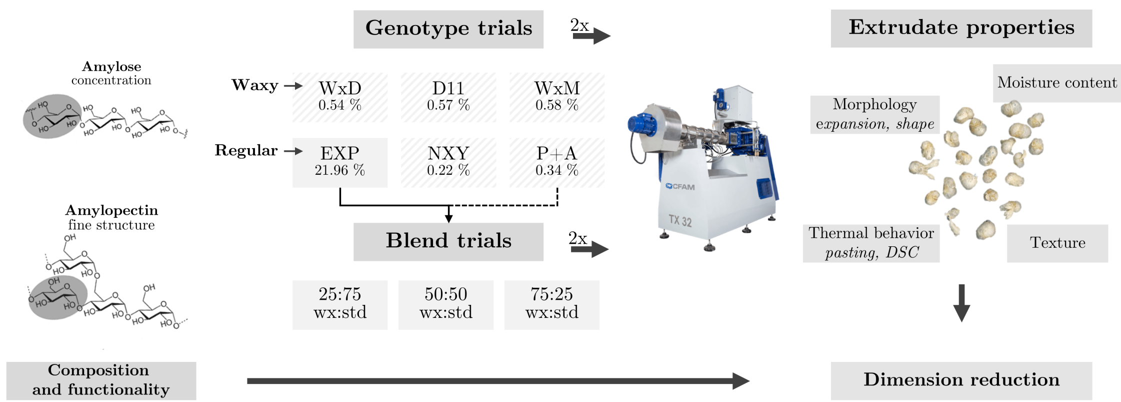

Graphical Abstract

Variation in amylose concentration to enhance wheat flour extrudability

T. Hellemans, H. Nekhudzhiga, F. Van Bockstaele, Y.J. Wang, M.N. Emmambux, M. Eeckhout

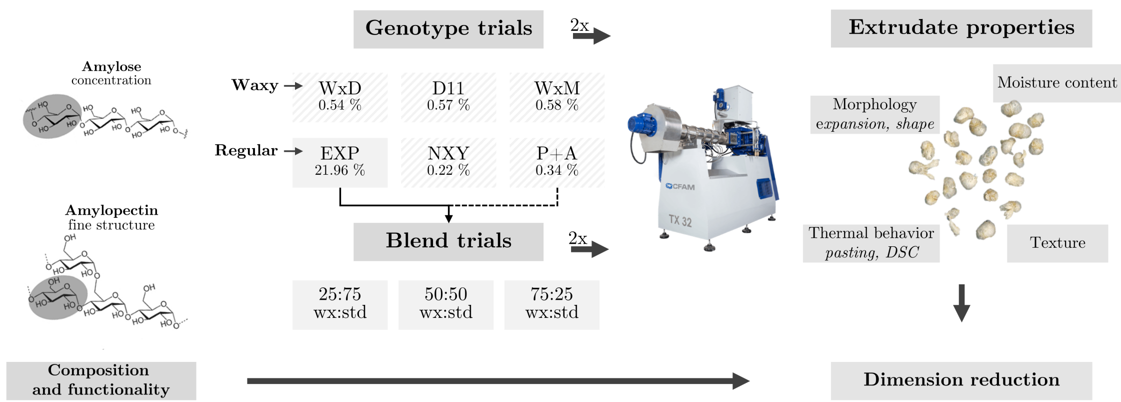

Highlights

Variation in amylose concentration to enhance wheat flour extrudability

T. Hellemans, H. Nekhudzhiga, F. Van Bockstaele, Y.J. Wang, M.N. Emmambux, M. Eeckhout

- Starch granule size distribution is related to extrudate texture.
- Amylose content affects expansion index, water absorption and texture of extrudates.
- Interaction between starch content and protein composition and quality was observed.
- Waxy genotypes are strongly varying in their protein composition and functionality.
- Maximum expansion was obtained for blends containing 25 % waxy flour.

Variation in amylose concentration to enhance wheat flour extrudability

T. Hellemans[a,*], H. Nekhudzhiga[c], F. Van Bockstaele[b], Y.J. Wang[d], M.N. Emmambux[c], M. Eeckhout[a]

[a] *Research unit on Cereal and Feed Technology, Department of Food technology, Safety and Health, Faculty of Bioscience Engineering, Ghent University, Ghent, Belgium*
[b] *Laboratory of Food technology and Engineering, Department of Food technology, Safety and Health, Faculty of Bioscience Engineering, Ghent University, Ghent, Belgium*
[c] *Department of Food and Consumer sciences Science, University of Pretoria, Pretoria 0002, South Africa*
[d] *Department of Food Science, University of Arkansas, Fayetteville, AR, USA*

Abstract

Composition and functionality of five waxy wheat (*Triticum aestivum* L.) genotypes were elaborately investigated and related to end-product attributes of extrudates. As such, the interaction between starch biopolymers and protein in extrusion processing could be studied. Furthermore, the effect of an increasing amylose-concentration was studied by the use of blends.

Waxy genotypes absorbed more water, gave rise to stiffer doughs and had higher onset and peak gelatinization temperature. In contrast, a lower pasting temperature and final viscosity and higher peak viscosity and breakdown could be observed. The volume percentage of small starch granules showed to be negatively correlated with peak temperature and positively with final viscosity and holding strength as well as with extrudate hardness. This was also positively correlated with amylose concentration. Expansion index was

*Correspondence: T.Hellemans@ugent.be; Tel.:+32-9-243-2494 (T.H.)

highest at a slightly decreased amylose concentration of 16.6 %. Markedly higher moisture content for all amylose-free extrudates was attributed to a combination of increased solubility of amylopectin and reduced water evaporation at die emergence. It was hypothesized that an interplay with protein content and composition was laying at the basis of the observed differences. Moreover, the altered pasting behavior of waxy wheat may enhance the extrudability of gluten containing wheat flour.

Keywords: waxy wheat, extrusion, pasting, starch fine structure

Declarations of interest: none

---

1. Introduction

The use of wheat (*Triticum aestivum* L.) for the production of foods for human and animal consumption is self-evident due to its global availability, a high yielding potential—with top producing countries such as Ireland (10.2 t/ha), New Zealand (9.9 t/ha), Belgium and the Netherlands (8.6 and 9.1 t/ha resp.)—and the unique viscoelastic properties (MacRitchie, 2016). Main applications of wheat are bakery products (bread, biscuits, *etc.*) that require a gluten network formation for which wheat flour has to be mixed with high amounts of water (50–65 % of the flour weight) (Barak et al., 2014; Hellemans et al., 2018). The gluten network provides a high gas retention capacity and a desirable crumb elasticity in the end-product. Extrusion processing, however, combines low water contents with a high temperature, shear rate and pressure, thereby partially abolishing the beneficial functional effects of gluten proteins. Earlier research found that both protein concentration and composition negatively affect extrudate properties such as the expansion index, water absorption and hardness (Hellemans, 2020). Pietsch et al. (2018) have shown that, on a molecular level, both the strong disulfide bond formation and hydrophobic interactions during twin-screw extrusion induce an intense polymerization of the wheat gluten. This prevents a proper expansion, thus resulting in dense and chewy instead of light and crisp extrudates. Moreover, an increased chance of blocking the extruder exists due to the high motor torques. For these reasons, mainly low quality (i.e. lower protein content) wheat cultivars are used in extrusion processing.

Nevertheless, besides protein properties, starch attributes may be employed to enhance processability and end-product quality due to the importance of both starch-starch and starch-protein interactions. For example, one of the main factors determining the extrudate properties is the melt viscosity (Robin et al., 2011) which, on its turn, has been related to the starch physicochemical properties (e.g. amylose:amylopectin-ratio, granule size distribution, presence of amylose-lipid complexes, etc.) and the starch pasting behavior (Kristiawan et al., 2018). Additionally, competition for water between protein and starch during extrusion further complexes these interactions.

In practice, the amylose content of conventional bread wheat is narrowly distributed between 25–28 %. Moreover, compared with waxy maize flour, (partial) waxy wheat flour is relatively new (Van Hung et al., 2006; Šárka and Dvoáček, 2017) and also high-amylose wheat flours (containing amylose contents up to 50–80 %) have only been commercially introduced in North America and Australia recently. Starch properties of waxy wheat flour may however provide possibilities to counteract the potential negative effects of the presence of wheat gluten proteins as it lowers the specific mechanical energy (SME) (Kowalski et al., 2015), thereby reducing the chance of ceasing the extruder. Moreover, they can also be used to obtain enhanced sensorial features or to produce high-energy foods at less demanding processing conditions due to the lower gelatinization temperature of waxy starches.

Results on the added value of waxy (wheat) flour to produce ready-to-eat (RTE) expanded snacks are however contradictory. The incorporation of waxy flour and hence, the lowering of the amylose content in the mix, had a main effect on the expansion of the extrudates. Some studies showed an increase (Kowalski et al., 2015) while in other, a decrease (Jongsutjarittam and Charoenrein, 2014; Thakur et al., 2017) in the expansion index (EI) was reported. In Jongsutjarittam and Charoenrein (2014), who compared waxy rice and rice flour based extrudates, this was attributed to the collapse during cooling. In addition, expansion was also impacted by the feed moisture content with an overall lower degree of shrinkage or collapse at high moisture contents. Despite the effects of amylose content on extrudate texture were related to differences in the EI, findings are also under discussion with both harder (Jongsutjarittam and Charoenrein, 2014) and softer (Kowalski et al., 2015) textures at lower amylose contents. As amylopectin is more sensitive to molecular degradation under extrusion conditions, waxy starches will show more short chain dextrins which lower the melt viscosity and thus, end-product properties such as the water absorption index (WAI) (Van Den Einde et al., 2004; Van den Einde et al., 2003). Under high-shear conditions (at high SMEs), molecular disruption was promoted in both regular and waxy barley flour leading to an increased WAI. This is supported by Jongsutjarittam and

Charoenrein (2014) who found that the entanglement of the linear amylose chains makes it more difficult to pull the network apart during expansion which implies the presence of intact (i.e. not (exo)degraded) polymers at increased SMEs. This network formation also resulted in a decreased EI for regular flour.

Vast amounts of research have already been performed on the relation between the amylose content and extrudate quality attributes, however, this was mainly done using rice or maize flour or starch. Kowalski et al. (2015) also stated that waxy *wheat* flours have not seen wide use in extrusion industry compared to other waxy flours (waxy maize and waxy barley). Moreover, previous studies frequently leave out intermediate amylose concentrations by studying the structure–functionality relationship using one or several pure waxy and regular cultivars. In bread, however, it has been proven that slightly reduced amylose concentrations increase end-product quality whereas 100 % waxy wheat significantly reduces structure and quality of the final product (Kowalski et al., 2015). The present work studies a range of amylose concentrations to provide additional insight in how amylose content influences end-product quality of wheat flour extrudates. Moreover, by screening multiple waxy cultivars, this study also broadens the knowledge on how genotype-dependent molecular differences may be deployed to improve waxy wheat flour applicability in extrusion processing.

2. Materials and methods

2.1. Raw materials

Five waxy wheat genotypes (table 1) were cultivated during 2017–2018 at the research farm of Ghent University and University College Ghent (Bottelare, Belgium). The field trial (Moortsele, Belgium, 50.96525 NB, 3.77977 EL) was conducted on a sandy loam soil with perennial rye grass as forefruit and was fertilized according to the advised dose rates for nitrogen (87 kg N ha^{-1}, 50 kg N ha^{-1} and 60 kg N ha^{-1} at Zadoks G.S. 22, G.S. 30 and G.S. 39, respectively). The harvested and cleaned wheat was tempered overnight to 15.5 % moisture and milled to flour using a Bühler laboratory mill. After a two week maturation period in plastic buckets at room temperature, flour samples were packed in polyethylene bags and were shipped to Pretoria (South Africa) for extrusion experiments. Regular wheat flour (so called *'Export flour'*) was obtained from Paniflower nv (Zwijnaarde, Belgium). This low-protein wheat flour ($<$10 %) contains no additives (e.g. vitamin C, enzymes, etc.) and is used as a reference flour throughout this research.

2.1.1. Formulation of blends

In this paper, results of two sets of extrusion trials are presented. In the blending trials (BT), the influence of the amylose content on extrusion properties and extrudate quality is studied. Therefore, waxy wheat flour (P+A) and standard bread wheat flour (EXP) were mixed in five different ratios: 100:0 (pure waxy wheat), 75:25, 50:50, 25:75, and 0:100 (pure regular wheat flour). In this way, amylose contents of approximately 0, 5.5, 11, 16.5 and 22 % were obtained. After weighing each flour in a separate bucket, a semi-industrial Hobart mixer equipped with a whisk was used to prepare homogeneous samples by mixing at low speeds for 10 minutes.

[Table 1 about here.]

2.2. Extrusion experiments

The expanded cereals were produced using a CFAM TX-32 laboratory scale co-rotating twin-screw extruder (CFAM Technologies (Pty) Ltd., Potchefstroom, South Africa). The extruder barrel consisted of five independent electrically heated and actively cooled zones. Prior to commencing the extrusion experiments, the die was preheated by the transferred heat of the fifth barrel zone. Barrel diameter D was 32.0 mm and barrel length L 500 mm (L/D-ratio = 15.65). A circular die (D = 3.0 mm) was used in combination with a single rotating knife. Results from preliminary trials were used to select suitable extruder operating conditions. Product feed rate (5 $kg\ h^{-1}$), water addition (0.28 $l\ h^{-1}$), screw speed (150 rpm), and temperature of zones 1–5 (40, 90, 100, 110, and 120 °C respectively) were kept constant during all trials. A conventional screw configuration consisting out of an initial conveying zone, two conveying and reaction zones (both ending with mixing elements), a single kneading block (for intense mixing during gelatinization) and a final conveying zone was used. All extrusion experiments were performed in duplicate in order to include processing variability in the statistical analysis.

To ensure uniform samples taking, an equilibration time of at least 4 minutes was set after changing the feed material. Both spherical extrudates

and strands were produced during each trial and were allowed to cool before packing them separately in hermetically sealed HDPE containers or PP bags. For the determination of the moisture content, the spherical extrudates were immediately packed in airtight HDPE containers without prior cooling.
A part of the collected and air-cooled extrudate was milled with an analytical mill (A11, IKA, Staufen, Germany) to pass through a 500 µm sieve. The samples were kept in polyethylene bags in an airtight container and stored at 4 °C until further analysis.

2.3. Raw material composition

2.3.1. Protein content

A VarioMax C/N (Elementar Analysesystemen GmbH., Langenselbold, Germany) was used to determine the nitrogen-content of the raw materials. Four hundred milligrams (as is) of each sample was accurately (precision of 0.1 mg) weighed in a crucible and placed in the autosampler. From the obtained nitrogen-content, the protein concentration was calculated using a conversion factor of 5.7. All protein contents presented in the manuscript are expressed on dry weight by using the raw materials moisture content, determined following AACCI Method 44-15.02.

2.3.2. Starch content, composition and structure

For the measurement of the granule size distribution of the starch, the amylose content and the starch fine structure, starch extracts were prepared from the wheat flour samples according to the method descirbed in Demeke et al. (1999) with slight adaptations (Hellemans, 2020).

Starch content. Starch content of the flour samples was measured in triplicate using the enzymatic method (K-TSTA) from Megazyme (Megazyme International, Wicklow, Ireland) following AACCI method 76-13.01.

Amylose content. The molecular size distribution of the starch was characterized using high-performance size exclusion chromatography. For debranched starch, 10 mg of starch was mixed with 3.2 mL of Millipore water, boiled for 30 min, cooled down and added with 0.4 mL of acetate buffer pH 3.5. Afterward, it was incubated with 10 µL of isoamylase at 45 °C for 2 h and then boiled for 15 min, and the buffer was removed with exchange resin IONAC NM-60 H^+/OH^--form, Type I (16-50 Mesh). The HPSEC system (Waters, Milford, MA) consisted of a 515 HPLC pump with a 200-µL sample loop, an in-line degasser, a 2410 refractive index detector maintained at 40 °C, and a series Shodex OHpak columns (KB-802 and KB-804) maintained at 55 °C. The effluent is 0.1 M $NaNO_3$ and 0.02% NaN_3 at an elution rate of 0.5 mL/min. Amylopectin (AMP) and amylose (AM) content were calculated from the area of their corresponding peaks by Empower Software.

Starch fine structure. Amylopectin chain-length distribution was characterized by high-performance anion-exchange chromatography with pulsed amperometric detection (HPAEC-PAD). A 10 mg defatted starch was mixed with 3.2 mL of deionized water, heated in a boiling water bath for 30 min, cooled to room temperature, and the pH adjusted with 0.4 mL of 0.1 M acetate buffer (pH 3.5). Ten µL (10 U) of isoamylase (Pseudomonas isoamylase, Megazyme International, Wicklow, Ireland) was added and the mixture was incubated in a water bath shaker at 45 °C with stirring at 150 rpm for 2 h. The pH of the mixture was neutralized by adding 0.21 mL of 0.2 M

NaOH, heated in a boiling water bath for 15 min, and allowed to cool at room temperature for 5 min. A 1.5 mL aliquot was centrifuged at 5000 × g for 5 min in a non-stick Eppendorf tube to remove insoluble materials. A 0.6 mL supernatant was used for the HPAEC-PAD analysis using a Dionex ICS-3000 ion chromatography system (Dionex Corporation, Sunnyvale, CA) with an AS40 automated sampler, a 50-mm CarboPac PA1 guard column, and a 250-mm CarboPac PA1 analytical column. Two eluent systems (150 mM NaOH and 500 mM $NaNO_3$ in 150 mM NaOH) were used to separate the branch-chain fractions by gradient elution. Sugars with DP 1 to 7 were used to identify the chromatographic peaks. The assignment for the chromatographic peaks with DP higher than 7 was based on the assumption that each successive peak represented a saccharide that was 1 DP longer than that of the previous peak. Duplicate measurements were taken for each starch sample.

2.3.3. Starch granule size

After starch extraction, granule size distribution was determined in aqueous conditions using a Mastersizer 2000S (Malvern Panalytica, Malvern, UK) equipped with a Hydro 2000S module. Directly after initiating the measurement, starch extract (12–18 mg) was suspended in 1 mL ultrapure water using a micropipette. The suspension was added to the dispersant (water) tank until an obscuration between 11 and 16 % was obtained. During the 75 s measuring cycle, three snapshots (technical repetitions) were taken. A general purpose analysis model was used with the particle refractive index and absorption indices of 1.53 and 0.1 respectively, while the refractive index of the dispersant was 1.33. Particle size is defined in terms of 10th percentile

(D_{10}), median (D_{50}), 90th percentile (D_{90}) and the relative contribution of B-type (≤10.0 µm) and A-type (10.01–35.0 µm) granules. The proportion of granules larger than 35 µm is denoted as 'A^{+}'.

2.4. Functional properties

2.4.1. Pasting behavior

Flour (both blends and the pure genotypes) and ground extrudates pasting behavior was measured using a Physica MCR 101 Rheometer (Anton Paar, Ostfildern, Austria) equipped with a starch pasting cell with a six-blade vane. Prior to commencing the pasting cycle, flour was mixed with 15 mL distilled water whereas the ground extrudate was added during the pre-shear phase (14 % w/v, 2.1 g on dry basis). This was done to ensure that all sample was added to the water. The pre-shear—a logarithmic increase to 960 rpm while heating to 50°C during a period of 30 s—was followed by stirring at 160 rpm throughout the entire measurement. A holding phase of 1 min at 50 °C was followed by a heating phase to 95 °C at 5 °C min^{-1}. Subsequently, a holding phase at 95 °C for 5 min and cooling phase (rate equal to heating phase) was completed. The measurement was ended by a final holding phase at 50 °C for 2 min.

From the recorded curves (minimum 3 repetitions per sample), the pasting and peak temperature (T_g, P_{temp}) were determined , as well as the viscosity at the peak (PV), during the holding period (holding strength, HS) and at the end of the measurement (final viscosity, FV). The breakdown (BD) and SB_{tot} were respectively calculated as the difference between PV or FV and HS.

2.4.2. Thermal analysis

Thermal properties of both the raw material (flour) and ground extrudates was determined in duplicate using a high-pressure differential scanning calorimeter (DSC) (HP DSC827e, Mettler Toledo, Greifensee, Switzerland). Approximately 10.0 ± 0.2 mg of sample (as is) was mixed with distilled water (40 mg) in 100mg DSC-pans. Prepared samples were left at least 24 h at room temperature to equilibrate. After calibrating the equipment with Indium (Tp = 156.6 °C, 28.455 $J.g^{-1}$), scanning was performed from 30–130 °C at a rate of 3.0 °C min^{-1}. All measurements were performed at a pressure of 4 MPa using N_2. An empty pan was used as a reference.

2.4.3. Flour water absorption

A Brabender Farinograph (Brabender Technologie GmbH, Duisburg, Germany) equipped with a 50 g mixing bowl was used for determining the optimal water absorption of the flour at 500 BU following ISO 5530-1:2013. Due to the limited amount of sample, the analysis was performed once.

2.4.4. Visco-elastic dough properties

Dough visco-elastic properties were measured for the various genotypes by means of a frequency sweep using an Anton Paar MCR 102 rheometer (Anton Paar, Ostfildern, Austria). The analysis was performed at least in triplicate. Dough pieces were obtained by mixing 10.0 grams of flour with 5.9 ml distilled water using the Glutomatic apparatus (Perten Instruments, Hägersten, Sweden). After mixing for one minute, the dough piece was carefully transported to the rheometer and the measurement was started. Prior to the frequency sweep, a 20 min relaxation period was set. The measurement itself was conducted at 20 °C going from 0.1–20 Hz at 250 Pa. From the obtained storage (G') and loss (G") modulus, the phase shift angle ($\tan(\delta)$) and the complex shear modulus ($|G^{*}|$) was calculated. Values at 10 Hz were used for further analysis.

2.5. Extrudate properties

2.5.1. Moisture content

Moisture content was determined in threefold on the spherical extrudates using samples which were collected directly at the extruder outlet and which were stored in hermetically sealed containers. Five to thirty extrudates were counted and weighed in aluminum crucibles and were dried in two stages: at 50 °C for 24 hours and at 130 °C for another 16 hours. After cooling to room temperature, the crucibles were again weighed on an analytical balance. Moisture loss was calculated as the relative weight difference. Based on the number of extrudates, the average weight per extrudate was as well determined.

2.5.2. Expansion-index and morphology

The expansion-index (EI) of the extrudates was determined by dividing the diameter of the strands (measured in tenfold with a caliper with a 0.1 mm accuracy) by the diameter of the die outlet (3.0 mm).
Morphological parameters (area size, length-to-width ratio and circularity) of the spherical extrudates (denoted as 'kernels') were determined using the SmartGrain image analysis software, version 1.2. Scans of 50 to 100 spherical extrudates were made using an Epson Perfection 2580 flatbed scanner (Seiko Epson, Nagano, Japan) against a blue background. After equally distribut-

ing the extrudates on the scanner surface, the lid was carefully put on top of the extrudates and a scan was made at 300 DPI. Raw, non-optimized, images were stored in the .jpeg file format (maximal quality level) with a resolution of 2550 × 3510 pix. After loading the files in the software, five random background areas and extrudate areas were selected for automated color thresholding. As the software was originally developed for grain kernel analysis, the option to substract the beard of the kernels was switched off.

2.5.3. Texture

Extrudate hardness was measured using a TX.XTplus Texture Analyzer (Stable Microsystems, Godalming, United Kingdom), mounted with a 50 kg (49 N) load-cell and aluminum circular probe (P/36R, D = 36 mm). A single spherical extrudate was positioned in the center of the test platform before starting the compression test. Extrudates were compressed at 2.00 $mm\ sec^{-1}$ for a distance of 5.000 mm. Pre- and post-test speeds were set at 12.000 $mm\ sec^{-1}$ and a trigger force of 0.3 kg (2.94 N) was used to initiate data recording. Per sample, 20 replicates were performed.

Using an in-house developed R-script (version 3.4.3), the breaking strength of the spherical extrudate was defined as the maximum force of the first peak which showed a 15 % loss in measured force over a 0.16 s interval (80 data points).

2.6. Statistical analyses

For data analysis, the R software package version 3.5.1 was used. Analysis of variance (ANOVA) was used to determine whether the main effects (genotype or blending ratio) and interaction effects were significant. Principal component analysis (PCA) using the compositional, functional and end-product quality attributes was executed to obtain insight in the variability in the dataset for the different genotypes. This aided in relating the raw material properties with extrudate quality parameters. To enhance data presentation, only the two first principal components were observed. Colors of the variable arrows represent the contribution of a variable to a given principal component (in percent).

3. Results

3.1. Raw materials

Sample composition was evaluated by means of analyzing the concentration of protein and starch while from the latter, also the composition (amylose content, amylopectin fine structure), and granule size distribution was studied. Furthermore, various functional properties such as the viscoelastic behavior (by means of dynamic oscillatory rheology) and the water absorption (using the Brabender Farinograph) of the flours were determined. The average values for these analysis are shown in table 2.

The protein content of all genotypes is remarkably low for bread wheat, varying from 9.7–11.7 %dm. This may be a direct result of the limited amounts of N fertilization applied during cultivation. Due to the short growing season of spring wheat genotypes (sown in April, harvested in July), P+A has a naturally high protein content. The phase shift angles ($\tan(\delta)$) and complex shear moduli ($|G^*|$) of all waxy samples, except D11, are highly comparable under the used test conditions. This indicates that the dough has comparable visco-elastic properties at 58 % hydration. On the contrary, values for the water absorption obtained using the Brabender Farinograph ranged from 62.5 to 71.6 % for D11 and NXY respectively.

Research from Zhang et al. (2014) attributed a varying water absorption to variation in the amylose concentration and the granule size distribution. Also TSt was related to WA although it was unclear if this was directly related to the starch or if this was an indirect effect of protein dilution (Purna et al., 2011). Starch contents were not significantly differing for the waxy genotypes with exception of P+A which had a lower starch concentration (76.8 $\pm$ 2.2). The amylose content of the regular wheat flour (EXP) (21.96 $\pm$ 0.73 %) is in accordance with the range reported by Van Hung et al. (2006) and concentrations in all waxy-cultivars was below 1 %. Minor variations within this group could be observed with contents ranging from 0.22 $\pm$ 0.01 to 0.58 $\pm$ 0.04 %.

For the amylopectin (AMP) branch chain length distribution, a significantly higher average chain length (aCL) (*i.e.* DP) was seen for WxD (DP = 20.79). EXP, on the contrary, had on average shorter AMP chains (aCL = 20.03). This distinction can be related to significant differences in the distribution pattern with lesser DP 6–24 chains and more long (DP 25–65) branches for the waxy wheat flours compared to regular wheat flour (Table 2). Presence of A-type (DP = 6–12) and B_3^+ (37–65) AMP chains was negatively correlated and showed the largest variation. For the A-type chains, WxD was significantly differing from D11 and P+A which were in turn significantly lower from EXP. An opposite trend was found for the B_3^+-chains. In addition, only EXP had a significantly higher proportion of B1-type chains (DP 13–24) whereas it had a lower amount of midlong (B_2-type, DP 25–36) chains. D11 and WxD had a significant higher concentration B_2-type chains. In general, an average relative proportion of 25.59, 47.55, 17.46 and 9.41 % was found for the different chain lengths (A, B_1, B_2, B_3^+-types, respectively).

Results for the starch granule size distribution were markedly different for all genotypes except WxD and D11 who showed similar trends. Besides the relation between granule size and flour water absorption (during mixing and pasting), $\tan(\delta)$ and ($|G^*|$) were found to increase for smaller granule sizes (Soh et al., 2006). However, no one-on-one correlations were observed between granule size properties and dough rheological attributes. In contrast, peak temperature in starch pasting measurements (P_{temp}) was significantly negatively correlated with the amount of B-type granules ($R^2 = 0.776$, $p = 0.048$) which might be related to their increased water absorption capacity as a result of the higher surface area to volume ratio.

[Table 2 about here.]

3.1.1. Thermal properties

In addition to the aforementioned functional properties, thermal properties of the flour (starch gelatinization and protein denaturation) was studied more in-depth by using pressurized DSC (limited amount of water) and viscosity measurements (starch pasting cell under constant stirring in excess of water). As extrusion processing partially remains a *black-box*, it is advantageous to gain a broad insight in the pasting behavior under both conditions.

DSC-profiles of the flour from the different genotypes all showed a single endotherm within a temperature range of 53.1–67.9 °C (table 2). EXP had the lowest onset (T_o) and peak (T_p) temperature (53.1 and 59.7 °C resp.)

and the second lowest endset temperature (T_e = 65.1 °C). Moreover, it was characterized by a low enthalpy (ΔH) of 2.7 $J.g^{-1}$. P+A, on the other hand, has the highest T_o (59.2 °C), T_p (63.8 °C), and T_e (67.9 °C). Both NXY and WxM, however, had higher enthalpies (6.9 $J.g^{-1}$ and 6.6 $J.g^{-1}$ resp.) compared to P+A (ΔH = 6.4 $J.g^{-1}$).

Ground extrudate powder was also subjected to DSC analysis, performed using the same methodology but did not show any significant endotherm over the entire scanning range (30–130 °C) (results not shown). This may indicate that no ungelatinized starch (i.e. intact granules) remains after extrusion cooking as was also reported by Ozcan and Jackson (2005).

Pasting profiles of the pure waxy wheat *flours* illustrate clear differences, mainly in the pasting temperature (T_g), peak viscosity (PV) and the peak temperature (P_{temp}). Genotypes WxD and D11 again show very similar trends analogous to the findings from the DSC measurements. NXY is characterized by the highest PV (3348 $\pm$ 16 mPa.s), followed by P+A (2537 $\pm$ 19 mPa.s), and WxD and D11 ($\approx$2123 mPa.s). WxM has a significantly lower PV of 1154 $\pm$ 39 mPa.s which also results in a significantly lower holding strength (HS) and final viscosity (FV) of 128 $\pm$ 3 and 190 $\pm$ 5 mPa.s respectively. This may be an effect of the high enzyme (α-amylase) activity in the sample, resulting in a breakdown of the starch at heating (results not shown). Additionally, P+A has a higher T_g of 65.7 °C compared to all other waxy flours of which the pasting temperature is approximately 60 °C. All parameters from the pasting curves can be found in table 3.

Figure 1**B** illustrates the consequences of blending flour to obtain a specific amylose content. The two distinct peaks at approximately 6 and 10 min, which are mainly visible in the curves with blending ratios 75:25, 50:50 and 25:75, are from the waxy wheat and regular wheat respectively. At decreasing blending ratios (towards pure regular wheat flour), the PV of the first peak will decline while the second peak increases in height. Nevertheless, the total AUC for the two first peaks appears to be relatively lower for the 50:50 and 25:75 wx:std blend compared to the expected peak area. Moreover, pure flours (both pure waxy [P+A]) and regular wheat flour [EXP]) have significantly higher FVs compared to the blends (586–678 mPa.s compared to 209–289 mPa.s). Amylose is crucial during network formation upon cooling as the long molecules can form a backbone in the starch-protein network although this is depending on the molecular weight of the molecules (Singh et al., 2009a). Various researchers observed a positive correlation between amylose content and FV although the interplay with proteins, lipids and non-starch polysaccharides contributed significantly to these effects. The similar high FV for both pure waxy and pure regular wheat flour may be attributed to the amylose-to-amylopectin-ratio and the ability of amylopectin molecules to aggregate via double helix formation in the absence of distorting elements (such as amylose) (Blazek and Copeland, 2008).

[Figure 1 about here.]

[Table 3 about here.]

3.2. Extrudate characteristics

Extrudate quality was evaluated by means of their moisture content and average kernel weight, morphological attributes and texture (i.e. hardness).

Results for both the genotype trials (GT) and blending trials (BT) are shown in table 4.

Moisture content of the extrudates shows to be significantly ($p<0.001$) influenced by the genotype with D11 having the highest value of 15.7 % while P+A has the lowest value (13.9 %) for the waxy genotypes. EXP differentiates with a very low extrudate moisture content of 10.6 %. This implies an effect of the amylose content on moisture loss during expansion at die emergence. Results from the BT confirm this with extrudates made from 100:0 Wx:std having a significantly ($p<0.001$) higher MC than 50:50 blends and, subsequently, regular wheat flour (13.9 %, 12.7 % and 10.6 % respectively). Despite minor variations between average kernel weights were recorded for the various genotypes—ranging from 0.166 $g/extrudate$ for D11 to 0.221 $g/extrudate$ for NXY—no influence of amylose content ($p=0.477$) was found.

When the melt exits the die, expansion occurs as a result of the flash evaporation of water resulting in 1) a reduction of the moisture content of the extrudate, 2) a rapid decrease of the melt temperature and, consequently, a solidification of the viscous structure. By dividing the resulting diameter of the extrudate (strands) by the diameter of the die (3.0 mm), the expansion-index (EI) is obtained. Although differences in the EI were limited (ΔEI $= 0.28$), a genotypic effect ($p<0.01$) could be observed. P+A and D11 had the highest EIs (3.97 $\pm$ 0.12 and 3.94 $\pm$ 0.20 resp.) while NXY being the least expanded (3.71 $\pm$ 0.30). Additionally, amylose contents significantly affected the EI, however, the correlation was not linear. The 25:75 blend resulted in the highest value (4.16) with a decrease towards higher incorporations of waxy wheat in the blends. Regular wheat flour had the lowest EI within the BT. This might possibly be due to a collapse of the gas cells just after expansion. Based on automated image processing of scans of the spherical extrudates, the morphology could be studied. Besides area, the length-to-width ratio (LtWr) and the circularity provide additional insight in the resistance of the extrudate against collapse after expansion. All three measures are showing a significant influence of the genotype ($p<0.001$), as well as from the amylose content (i.e. blending rate) ($p<0.001$). The area size is the smallest for WxD and D11 which are both significantly differing from NXY and WxM. P+A and EXP have the highest area size. Despite the significantly lower area size for NXY-based extrudates compared to those of EXP and P+A (108 ± 18 *versus* 130 ± 26 and 126 ± 20), the LtWr and circularity of the former genotype is (almost) equal to EXP and P+A. Results from the BT clearly indicate an optimum for both LtWr and circularity at a blending ratio of 75:25 wx:std. Both lower and higher amylose contents result in increased widths, thus, decreased circularity. For the area size, no clear trend of amylose concentration was observed.

[Table 4 about here.]

Extrudate texture (i.e. crispness) is an important quality attribute for expanded *ready-to-eat* snacks as it is typical for this type of products. Despite crispness, as a sensorial parameter, can be defined in various different ways, hardness and compression distance at which the outer layer of the extrudate breaks are known to be a good indicators. Clear genotypic effects for both the hardness and compression distance are observed ($p<0.001$) with WxM and EXP having an average higher breaking strength (25.997 ± 9.575 N and 2.623 ± 0.626 N resp.) compared to all other genotypes ranging from 18.688 ± 6.043 to 21.396 ± 11.085 N). However, for the compression distance, EXP is significantly differing from all waxy genotypes. This means that, before breaking occurs, extrudates from EXP have to be compressed to a larger extent (0.76 ± 0.34 cm compared to 0.46 ± 0.24 cm), indicating that extrudates made from waxy wheat flour are more brittle. Analogues to the findings from the genotype trial, a clear effect of the amylose content on both hardness and compression distance is found ($p<0.001$). Both factors steadily increased respectively from 18.688 to 25.732 N and 0.39 to 0.77 mm upon increasing amylose concentrations (lower percentage waxy wheat flour). On the basis of the BT it was observed that extrudates produced with pure waxy wheat flour needed 7.044 N less compression force than extrudates made from regular wheat flour.

3.3. Pasting behavior

In order to obtain an insight in the water binding capacity and the presence of intact (i.e. unpasted) starch after extrusion cooking, the pasting behavior of the ground extrudates was determined. The resulting curves for both the GT and BT can be found in figure 1.

As the ground extrudate was added to the distilled water during the preshear phase, a first peak occurs at the beginning of the diagram as a result of the hydration of the starch components (amylose, amylopectin and fragmentated polysaccharides) in the extrudate. For the PV, genotypes P+A (73.2 ± 3.7 mPa.s) and WxM (75.5 ± 3.5 mPa.s) have lower values than

D11 and WxD (93.9 ± 2.4 and 98.0 ± 6.1 mPa.s resp.). Overall, viscosities remain quite low. During the heating phase, at 93.8 and 94.2 °C respectively, WxD and P+A show a small viscosity increase (first arrow around minute 11) whereas all other genotypes evolve towards a stable viscosity during the holding phase at 95 °C. These two genotypes also show a drop in their viscosity during cooling (second arrow at 23 minutes) making them return towards the expected viscosity range. FVs range from 79.0± 2.0 to 89.0 ± 5.2 mPa.s, following the same order as with the viscosity of the primary peak.

Samples from the BT only show an initial peak at the hydration of the powder (PV) as is illustrated in figure 1**B**). The effect of the amylose content in the extrudates clearly comes to expression in these pasting curves. PV values increase in an exponential way ($R^2 = 0.998$) from 74 ± 3 to 556 ± 42 mPa.s.

4. Discussion

The variation in the protein properties (both content and composition) of the wheat flour from the different genotypes may have influenced the end-product quality of the extrudates, mainly the expansion index (EI), as reported in previous research (Hellemans, 2020). In general, expansion will decrease at increasing protein concentrations with fewer but larger gas cells at high (>16 %) wheat gluten enrichment. In addition, this was found to be dependent on the composition of the (gluten) proteins as a result of their botanical origin (e.g. soy or wheat proteins), the genotype and the growth conditions. On the contrary, compared to pure wheat starch, addition of wheat gluten showed to have a stabilizing effect on gas cell formation (in terms of obtaining a more homogeneous internal structure in the extrudates) implying that an optimum for EI in function of protein content exists (Moraru and Kokini, 2003; Draganovic et al., 2013).

A positive correlation (p=0.03, R^2=0.715) between dynamic rheological parameter $|G^*|$ and farinograph water absorption could be observed. However, this result was in contrast with Van Bockstaele et al. (2008), who has reported a *negative* correlation of R^2=0.548. This difference can be explained by the use of a fixed water addition in the current study while Van Bockstaele et al. (2008) used 95 % of the optimal WA. Water is an important factor in determining the viscoelastic properties of dough as it has a dual role as inert filler and lubricant. In this study, an increase in the $|G^*|$ resembles a higher resistance to deformation as a result of different water absorptions of the flour constituents (mainly proteins and starch). Although $|G^*|$ and $\tan(\delta)$ may be valuable for predicting extrudate properties (*eg.* expansion and hardness), it can be argued that correlations between $|G^*|$ or $\tan(\delta)$ and end-product characteristics are lacking as during measurements, forces within the LVR were applied. Van Bockstaele et al. (2008), however, found a strong correlation ($R^2 = 0.74$) between $|G^*|$ and the bread volume. Kristiawan et al. (2016) hypothesized that these parameters could provide insight in the visco-elastic behavior of the melt (mainly the storage modulus) during extrusion which, on its turn, has been related to macroscopic expansion behavior. Relations are however not straight-forward as the latter is obtained through a complex combination of nucleation, bubble growth, coalescence, shrinkage and fixation.

Granule size distributions are strongly differing for the different genotypes which may affect starch gelatinization both in excess of water as well as during extrusion processing. As investigated by Singh et al. (2009b), starch rheology is mainly influenced by particle size whereby suspensions of large size particles tend to be more viscous compared to those of the counterpart smaller size (i.e. A and B-type granules respectively). In this study, the relative proportion of B-type granules ($\leq$10 µm) showed a significant negative correlation with the pasting temperature (T_g) ($p \leq 0.05$, R^2=0.776) whereas, for A-type granules (10–30 µm), positive correlations ($p \leq 0.05$) with the holding strength (HS) (R^2=0.815) and final viscosity (FV) (R^2=0.831) were found. The latter finding is in accordance with results from Kumar and Khatkar (2017) and can be attributed to the occupation of a relatively larger volume in the solution compared to B-granules at a similar quantity. Increased interaction between surfaces of unpasted (remnants of) starch granules after reaching the peak viscosity will thus contribute to a higher HS and FV (Hellemans et al., 2017). Also, the decrease in peak viscosity (PV) and the generally lower FV for the EXP flour compared to waxy flours was related to an increase in amylose content (Singh et al., 2009b; Kumar and Khatkar, 2017; Zi et al., 2019).

By means of principal component analysis (PCA), compositional and functional attributes of the raw materials and quality characteristics of the extrudates were related. In total, 68.9 % of the variance in the dataset could be explained by the two first PCs (figure 2). Colors of the arrows indicate the contribution of each variable going from dark blue (low) to dark red (high). The first PC (PC1, 45.3 %) is mainly correlated with starch related attributes such as TSt, granule size distribution parameters and thermal properties

(DSC and pasting) whereas the second PC (PC2, 22.1 %) resembles protein properties (farinograph water absorption, $|G^*|$ and $\tan(\delta)$).

[Figure 2 about here.]

Water absorption (WA) is negatively correlated with the expansion index ($R^2 = 0.90$) of the extrudates as well as with $|G^*|$ ($R^2 = 0.71$) and, to a lesser extend, $\tan(\delta)$ ($R^2 = 0.58$). In addition, MC of the extrudates is negatively correlated with both PV and protein content (PRO). This may be related to the increased hydrophobicity of proteins after extrusion (Wagner et al., 2011) resulting in a increased moisture loss at higher PRO. These findings also indicate the importance of PRO and composition in determining the visco-elastic behavior of the melt and, eventually, the expansion of the extrudates and the accompanying moisture loss at die emergence.

Firstly, increased molecular degradation (depolymerization and debranching) of amylopectin during extrusion of waxy wheat (Ozcan and Jackson, 2005) may result in an elevated moisture loss through evaporation as the formed gluten-starch network will have a lower water binding capacity. However, depolymerized amylopectin—occuring mainly at the $\alpha(1\rightarrow6)$-bonds—will result in an increased solubility of the obtained components (short chains), thereby promoting water binding. Moreover, as AMP contents are not significantly differing for the different genotypes, its contribution is considered to be limited. In contrast, limited network formation by the entanglement of these short amylopectin chains may decrease gel strength (Blazek and Copeland, 2008), thus promoting rupturing upon fast expansion during flash evaporation. This will also be highly dependent from the protein properties.

An increase in the protein content may improve gas cell formation by the development of a strong but flexible gluten-starch film around the gas cells (Sroan et al., 2009). Its strength is also determined by the protein composition, primarily the content of high molecular weight proteins (i.e. HMW-GS). As reported by Purna et al. (2011), gas cell formation during breadmaking also requires a good balance between elasticity and extensibility to allow the gas cells to expand and to rupture, thus enabling vapor to go out of the product. Another hypothesis is that an increased expansion promotes evaporation due to a larger contact surface. The finding is, however, contrasted by the positive correlation with both the amylose content and amylopectin average chain length. As amylopectin degradation occurs mainly at the $\alpha 1 \rightarrow 6$ bonds, it seems unlikely that water binding lies at the basis of this effect.

Both TSt and the D90 (or alternatively the proportion of A- and B-type granules) are positively correlated with extrudate hardness. Based on various research outcomes, both parameters will influence melt viscosity which was related with extrudate hardness by Zhang et al. (2016). They have stated that the thermal properties (mainly ΔH) can affect the textural characteristics of the extrudates by influencing both the specific mechanical energy and the melt viscosity. However, it has to be kept in mind that, on one hand, the melt viscosity should be low enough to promote bubble growth but, on the other hand, should be high enough to prevent bubble collapse and coalescence. Lower viscosity can lead to decreased melt strength and increase the chance of gas cell collapse (Kristiawan et al., 2016).

When studying different genotypes with an altered composition in terms of protein and starch, a broad screening of all molecular and macromolecular attributes should be attained to properly investigate the possible protein-starch interactions determining in extrudate quality. In addition, an enhanced simulation of the pasting behavior of the flour during extrusion (under high pressure, shear and temperature and at low moisture contents) or on-line viscosity measurements should be included. Inherent to the use of blends to study the effect of a single attribute is the undesirable shift in other compositional properties (in this case: protein content and composition). A possible solution would be the use of near-isogenic lines.

5. Conclusion

This study has shown that, when applying waxy wheat flour in extrusion processing, an important genetic factor should be taken into account as both protein and starch related attributes influence its processability and thus, end-product quality. Nevertheless, a minimal addition of waxy wheat flour to regular wheat flour (25:75 wx:std) enhances the expansion ratio of the extrudate while resulting in more brittle products with an overall lower hardness. Effects are however not linear with the amylose-to-amylopectin ratio and the protein composition (and their mutual interaction) being crucial factors which should be taken into consideration when assessing the relation between composition and end-product quality. Results showed that also starch granule size distribution influences the pasting and gelatinization behavior, although the primary effect may remain the starch composition as this is found to be related with the size distribution pattern. Contrastingly, no clear evidence of a relation between the average amylopectin chain length and extrudate quality was found although waxy genotypes in this study had a higher proportion short branch-chains resulting in a significantly lower average chain length.

When studying different genotypes with an altered composition in terms of protein and starch, a broad screening of all molecular and macromolecular attributes should be attained to properly investigate the possible protein-starch interactions which are determining for extrudate quality. In addition, an enhanced simulation of the pasting behavior of the flour during extrusion (under high pressure, shear and temperature and at low moisture contents) or on-line viscosity measurements should be included. An improved understanding of both the factors influencing melt viscosity as well as how this is related to end-product quality is highly recommendable. This would however require a mechanistic modeling approach.

Inherent to the use of blends to study the effect of a single attribute, is the undesirable shift obtained for other compositional properties (in this case: protein content and composition). A possible solution to overcome these secondary effects would be the use of near-isogenic lines. The added value of using lines with a similar genetic background in this type of research did already come to expression through the highly comparable results observed for WxD and D11 which are known to be closely related.

6. Acknowledgments

This research was financially supported by the FWO, Research Foundation Flanders (Grant number 1S 609 16N) and VLIR-UOS Global Minds (grant number: BE2017GMUUG0A103). Special thanks goes to the University of Pretoria (South Africa) for facilitating the extrusion experiments as well as to prof. Ravindra N. Chibbar from the University of Saskatchewan (Saskatoon, Canada) for the determination of the starch granule size distribution.

References

Barak, S., Mudgil, D., Khatkar, B.S., 2014. Influence of Gliadin and Glutenin Fractions on Rheological, Pasting, and Textural Properties of Dough. International Journal of Food Properties 17, 1428–1438. URL: https://doi.org/10.1080/10942912.2012.717154, doi:10.1080/10942912.2012.717154.

Blazek, J., Copeland, L., 2008. Pasting and swelling properties of wheat flour and starch in relation to amylose content. Carbohydrate Polymers 71, 380–387.

Demeke, T., Hucl, P., Abdel-Aal, E.S., Båga, M., Chibbar, R., 1999. Biochemical characterization of the wheat waxy a protein and its effect on starch properties. Cereal Chemistry 76, 694–698.

Draganovic, V., Van Der Goot, A., Boom, R., Jonkers, J., 2013. Wheat gluten in extruded fish feed: effects on morphology and on physical and functional properties. Aquaculture Nutrition 19, 845–859.

Van den Einde, R., Van der Goot, A., Boom, R., 2003. Understanding molecular weight reduction of starch during heating-shearing processes. Journal of Food Science 68, 2396–2404.

Hellemans, T., 2020. Outline of four degrees of diversification for understanding bread wheat (Triticum aestivum L.) quality. Ph.D. thesis. Ghent University.

Hellemans, T., Abera, G., De Leyn, I., Van der Meeren, P., Dewettinck, K., Eeckhout, M., De Meulenaer, B., Van Bockstaele, F., 2017. Composition, granular structure, and pasting properties of native starch extracted from plectranthus edulis (oromo dinich) tubers. Journal of Food Science 82, 2794–2804.

Hellemans, T., Landschoot, S., Dewitte, K., Van Bockstaele, F., Vermeir, P., Eeckhout, M., Haesaert, G., 2018. Impact of crop husbandry practices and environmental conditions on wheat composition and quality: a review. Journal of Agricultural and Food Chemistry 66, 2491–2509.

Jongsutjarittam, O., Charoenrein, S., 2014. The effect of moisture content on physicochemical properties of extruded waxy and non-waxy rice flour. Carbohydrate Polymers 114, 133–140.

Kowalski, R.J., Morris, C.F., Ganjyal, G.M., 2015. Waxy soft white wheat: extrusion characteristics and thermal and rheological properties. Cereal Chemistry 92, 145–153.

Kristiawan, M., Chaunier, L., Della Valle, G., Ndiaye, A., Vergnes, B., 2016. Modeling of starchy melts expansion by extrusion. Trends in Food Science & Technology 48, 13–26.

Kristiawan, M., Micard, V., Maladira, P., Alchamieh, C., Maigret, J.E., Réguerre, A.L., Emin, M.A., Della Valle, G., 2018. Multi-scale structural changes of starch and proteins during pea flour extrusion. Food Research International 108, 203–215.

Kumar, R., Khatkar, B., 2017. Thermal, pasting and morphological properties of starch granules of wheat (triticum aestivum l.) varieties. Journal of Food Science and Technology 54, 2403–2410.

MacRitchie, F., 2016. Seventy years of research into breadmaking quality. Journal of Cereal Science 70, 123–131.

Moraru, C., Kokini, J., 2003. Nucleation and expansion during extrusion and microwave heating of cereal foods. Comprehensive Reviews in Food Science and Food Safety 2, 147–165.

Ozcan, S., Jackson, D.S., 2005. Functionality behavior of raw and extruded corn starch mixtures. Cereal Chemistry 82, 223–227.

Pietsch, V.L., Karbstein, H.P., Emin, M.A., 2018. Kinetics of wheat gluten polymerization at extrusion-like conditions relevant for the production of meat analog products. Food Hydrocolloids 85, 102–109.

Purna, S.K.G., Miller, R.A., Seib, P.A., Graybosch, R.A., Shi, Y.C., 2011. Volume, texture, and molecular mechanism behind the collapse of bread made with different levels of hard waxy wheat flours. Journal of Cereal Science 54, 37–43.

Robin, F., Bovet, N., Pineau, N., Schuchmann, H.P., Palzer, S., 2011. Online shear viscosity measurement of starchy melts enriched in wheat bran. Journal of Food Science 76, E405–E412.

Šárka, E., Dvoáček, V., 2017. New processing and applications of waxy starch (a review). Journal of Food Engineering 206, 77–87.

Singh, N., Singh, S., Isono, N., Noda, T., Singh, A.M., 2009a. Diversity in amylopectin structure, thermal and pasting properties of starches from wheat varieties/lines. International Journal of Biological Macromolecules 45, 298–304.

Singh, S., Singh, N., Isono, N., Noda, T., 2009b. Relationship of granule size distribution and amylopectin structure with pasting, thermal, and retrogradation properties in wheat starch. Journal of Agricultural and Food Chemistry 58, 1180–1188.

Soh, H., Sissons, M., Turner, M., 2006. Effect of starch granule size distribution and elevated amylose content on durum dough rheology and spaghetti cooking quality. Cereal Chemistry 83, 513–519.

Sroan, B.S., Bean, S.R., MacRitchie, F., 2009. Mechanism of gas cell stabilization in bread making. i. the primary gluten–starch matrix. Journal of Cereal Science 49, 32–40.

Thakur, S., Singh, N., Kaur, A., Singh, B., 2017. Effect of extrusion on physicochemical properties, digestibility, and phenolic profiles of grit fractions obtained from dry milling of normal and waxy corn. Journal of Food Science 82, 1101–1109.

Van Bockstaele, F., De Leyn, I., Eeckhout, M., Dewettinck, K., 2008. Rheological properties of wheat flour dough and their relationship with bread volume. ii. dynamic oscillation measurements. Cereal Chemistry 85, 762–768.

Van Den Einde, R., Akkermans, C., Van Der Goot, A., Boom, R., 2004. Molecular breakdown of corn starch by thermal and mechanical effects. Carbohydrate Polymers 56, 415–422.

Van Hung, P., Maeda, T., Morita, N., 2006. Waxy and high-amylose wheat starches and flours, characteristics, functionality and application. Trends in Food Science & Technology 17, 448–456.

Wagner, M., Morel, M.H., Bonicel, J., Cuq, B., 2011. Mechanisms of heat-mediated aggregation of wheat gluten protein upon pasta processing. Journal of Agricultural and Food Chemistry 59, 3146–3154.

Zhang, H., Zhang, W., Xu, C., Zhou, X., 2014. Studies on the rheological and gelatinization characteristics of waxy wheat flour. International Journal of Biological Macromolecules 64, 123–129.

Zhang, W., Li, S., Zhang, B., Drago, S.R., Zhang, J., 2016. Relationships between the gelatinization of starches and the textural properties of extruded texturized soybean protein-starch systems. Journal of Food Engineering 174, 29–36.

Zi, Y., Shen, H., Dai, S., Ma, X., Ju, W., Wang, C., Guo, J., Liu, A., Cheng, D., Li, H., et al., 2019. Comparison of starch physicochemical properties of wheat cultivars differing in bread-and noodle-making quality. Food Hydrocolloids 93, 78–86.

List of Figures

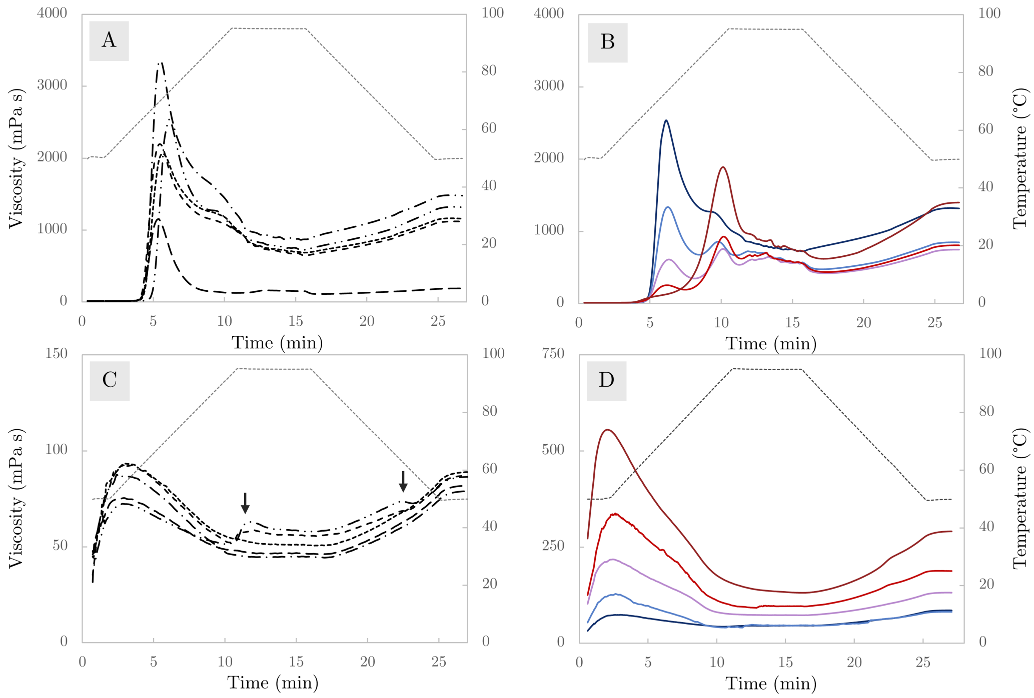

Figure 1: Pasting profiles of pure waxy wheat flours (**A**) and extrudates (**C**) (WxD - - , D11 ---, WxM ········, NXY -·-, P+A -··-) and blends of waxy and regular wheat flour (**B**) and the resulting extrudates (**D**) (100:0 wx:std —, 75:25 —, 50:50 —, 25:75 —, 0:100 —, temperature ·······).

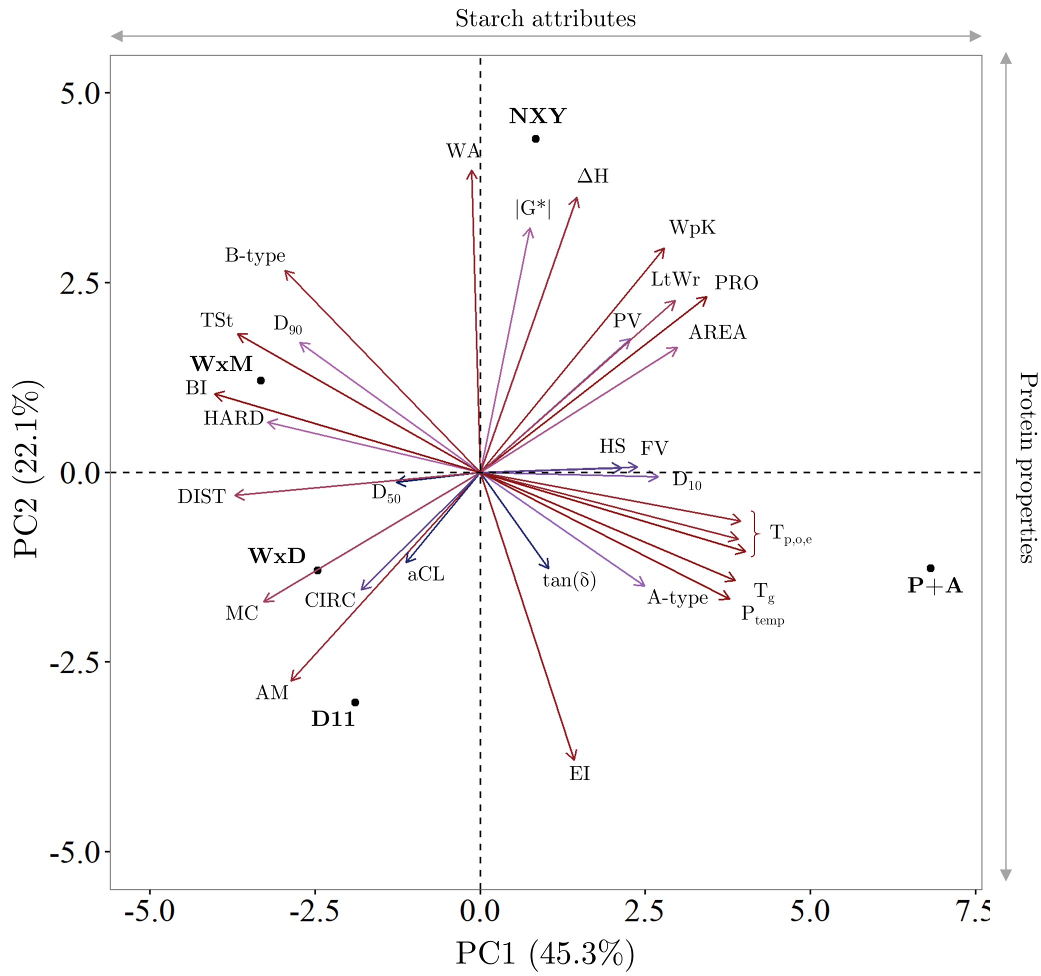

Figure 2: Biplot from the two first principal components (PC), together explaining 67.4 % of the variance in the dataset, based on compositional, functional and end-product quality attributes of the samples used in the genotype trial. The color of the arrows indicate the contribution—from dark blue (low contribution) to dark red (high contribution)—of each variable to the PCA.

List of Tables

Table 1: Overview of the wheat genotypes used in the experiments

Genotype	Owner	Origin	Wheat type	Code
WaxyDie	Dieckmann Seeds	Research farm	Winter wheat	WxD
1154.06	Dieckmann Seeds	Research farm	Winter wheat	D11
Waxymum	Limagrain Céréales Ingrédients SAS	Research farm	Winter wheat	WxM
NX12Y48222	USDA ARS (Bob Graybosch)	Research farm	Winter wheat	NXY
Penawawa+Alpowa	Washington State University (Craig Morris)	Research farm	Spring wheat (blend)	P+A
Export flour	Brabomills nv. (Paniflower)	Commercial flour	Unknown (blend)	EXP

Table 2: Composition and functionality of the raw materials (waxy flours and reference flour).

		WaxyDie	**1154.06**	**Waxymum**	**NX12Y48222**	**Penawawa+Alpowa**	**Waxy flours[2]**	**Export flour**
Composition	*PROC* (%dm)	9.7 ± 0.0	10.0 ± 0.0	10.2 ± 0.0	11.7 ± 0.0	11.7 ± 0.0	10.7 ± 1.0	9.7 ± 0.01
	TSt (% dm)	80.5 ± 4.2	80.8 ± 0.8	81.6 ± 2.6	81.6 ± 1.8	76.8 ± 2.2	80.3 ± 2.0	na
	AM (%)	0.54 ± 0.04	0.57 ± 0.12	0.58 ± 0.08	0.22 ± 0.01	0.34 ± 0.03	0.45 ± 0.16	21.96 ± 0.73
	AMP A (%)	24.60 ± 0.06	25.19 ± 0.19	25.77 ± 0.18	25.71 ± 0.09	25.53 ± 0.24	25.36 ± 0.46	26.73 ± 0.17
	AMP B_1 (%)	47.36 ± 0.08	47.56 ± 0.17	47.18 ± 0.25	47.48 ± 0.06	47.41 ± 0.11	47.40 ± 0.20	48.28 ± 0.08
	AMP B_2 (%)	18.37 ± 0.00	17.99 ± 0.06	17.33 ± 0.13	17.27 ± 0.20	17.41 ± 0.25	17.67 ± 0.46	16.39 ± 0.11
	AMP B_3^+ (%)	9.68 ± 0.02	9.26 ± 0.04	9.71 ± 0.06	9.53 ± 0.06	9.65 ± 0.10	9.57 ± 0.18	8.60 ± 0.02
	AMP aCL (%)	20.79 ± 0.01	20.53 ± 0.01	20.58 ± 0.02	20.53 ± 0.02	20.58 ± 0.08	20.60 ± 0.11	20.03 ± 0.01
	D_{10} (µm)	9.2 ± 0.1	1.2 ± 0.3	4.7 ± 0.1	5.4 ± 0.1	11.4 ± 0.0	8.2 ± 2.9	na
	D_{50} (µm)	20.8 ± 0.1	22.6 ± 0.3	20.5 ± 0.1	21.9 ± 0.1	20.3 ± 0.0	21.2 ± 1.0	na
	D_{90} (µm)	39.6 ± 0.2	46.6 ± 1.1	45.5 ± 0.2	47.0 ± 0.1	35.7 ± 0.0	42.9 ± 5.0	na
	B-type (%)	11.8 ± 0.2	9.7 ± 0.5	19.7 ± 0.3	15.3 ± 0.2	5.5 ± 0.0	12.4 ± 5.4	na
	A-type (%)	72.8 ± 0.1	68.5 ± 0.4	60.4 ± 0.1	63.0 ± 0.2	83.5 ± 0.0	69.7 ± 9.1	na
	A^+ (%)	15.4 ± 0.1	21.8 ± 0.9	19.8 ± 0.6	21.6 ± 0.2	11.0 ± 0.2	17.9 ± 4.66	na
Functional properties	*Water absorption*[1] (%)	65.9	62.5	65.7	71.6	63.9	65.9 ± 3.5	60.1
	tan(δ) (rad)	0.30 ± 0.01	0.33 ± 0.01	0.33 ± 0.00	0.31 ± 0.01	0.32 ± 0.01	0.32 ± 0.01	0.36 ± 0.01
	$\|G^*\|$ (MPa)	264 ± 29	164 ± 10	266 ± 62	288 ± 66	255 ± 42	247 ± 48	150 ± 9
	T_o (°C)	56.0	56.9	56.6	56.7	59.2	57.1 ± 1.2	53.1
	T_p (°C)	60.0	61.5	60.7	61.4	63.8	61.5 ± 1.4	59.7
	T_e (°C)	65.0	65.7	65.1	65.5	67.9	65.8 ± 1.2	65.1
	ΔH (Jg^{-1})	5.4	5.4	6.6	6.9	6.4	6.1 ± 0.7	5.4

tan(δ), phase shift angle; $|G^*|$, complex shear modulus; TSt, total starch; AM, amylose content; aCL, average branch-chain length of amylopectin; D_i, i^{th} percentile of the granule size distribution; $T_{o,p,e}$, onset, peak and endset temperature; ΔH, enthalpy

[1]Water absorption at 500 BU as determined by Brabender Farinograph

[2]Mean ± stdev for waxy cultivars

Analysis of variance (ANOVA) was not performed as mean and standard deviation are based on three values (n=3)

Table 3: Overview of the results from the starch pasting behavior of flour from pure genotypes and blends (14 %db) using a Physica MCR 101 rheometer (Anton Paar, Ostfildern, Austria)

Genotype	**T**$_g$ (°C)	**PV** (mPa.s)	**P**$_{temp}$ (°C)	**HS** (mPa.s)	**BD** (mPa.s)	**FV** (mPa.s)	**SB**$_{tot}$ (mPa.s)
WaxyDie	59.3 ± 0.0	2189 ± 52	69.8 ± 0.6	664 ± 4	1525 ± 48	1120 ± 4	456 ± 8
1154.06	60.2 ± 0.0	2056 ± 10	71.2 ± 0.0	692 ± 16	1364 ± 6	1158 ± 4	466 ± 12
Waxymum	59.3 ± 0.0	1154 ± 39	69.4 ± 0.0	128 ± 3	1026 ± 36	190 ± 5	62 ± 1
NX12Y48222	59.3 ± 0.0	3348 ± 16	70.3 ± 0.0	860 ± 3	2488 ± 19	1480 ± 11	620 ± 8
mean	59.5	2187	70.2	586	1601	987	401
stdev	0.5	900	0.8	317	627	555	238
100:0 wx:std	65.7 ± 0.0	2537 ± 19	73.1 ± 0.0	732 ± 4	1804 ± 22	1318 ± 4	586 ± 8
75:25 wx:std	65.7 ± 0.0	1335 ± 10	74.0 ± 0.0	559 ± 3	777 ± 13	848 ± 7	289 ± 8
50:50 wx:std	65.7 ± 0.0	610 ± 31	74.0 ± 0.0	537 ± 27	219 ± 13	746 ± 7	209 ± 34
25:75 wx:std	65.7 ± 0.0	259 ± 1	79.0 ± 7.2	565 ± 0	364 ± 24	808 ± 64	243 ± 64
0:100 wx:std	80.1 ± 0.5	1891 ± 78	93.0 ± 0.0	722 ± 14	1169 ± 65	1400 ± 131	678 ± 120

T_g, pasting temperature; PV, peak viscosity; P_{temp}, peak temperature; HS, holding strength; BD, breakdown (PV-HS); FV, final viscosity; SB_{tot}, total setback (FV-HS)

PV is defined as the y-value of the peak during the first heating phase or, if no peak is present, the first peak during the subsequent holding phase.

BD is calculated as the difference between the y-value (viscosity) of the highest peak and the HS.

analysis of variance was not performed as mean and standard deviation are based on three values (n=3)

Table 4: Quality attributes of extrudates from genotype trials and blend trials

Genotype	**MC** (%)	**WpK** (g)	**EI**	**Area** (mm^2)	**LtWr**	**Circularity**	**Hardness** (N)	**Distance** (mm)	**BI**[1] (%)
WaxyDie	14.9 ± 0.6^{ab}	0.188 ± 0.008^{c}	3.85 ± 0.24^{ab}	94 ± 15^{c}	1.20 ± 0.13^{d}	0.814 ± 0.050^{a}	21.396 ± 11.085^{ab}	0.51 ± 0.25^{b}	3.8
1154.06	15.7 ± 0.1^{a}	0.166 ± 0.014^{d}	3.94 ± 0.22^{a}	84 ± 17^{d}	1.26 ± 0.19^{c}	0.789 ± 0.085^{ab}	21.141 ± 9.879^{ab}	0.48 ± 0.25^{b}	3.9
Waxymum	14.8 ± 0.4^{bc}	0.197 ± 0.005^{bc}	3.84 ± 0.17^{c}	112 ± 20^{b}	1.31 ± 0.13^{b}	0.804 ± 0.048^{b}	25.997 ± 11.085^{a}	0.46 ± 0.28^{b}	4.3
NX12Y48222	14.5 ± 0.6^{bc}	0.220 ± 0.004^{a}	3.71 ± 0.30^{b}	108 ± 19^{b}	1.36 ± 0.15^{a}	0.781 ± 0.065^{c}	20.297 ± 10.379^{ab}	0.46 ± 0.23^{b}	3.8
mean	14.9	0.193	3.84	99	1.28	0.797	23.052	0.455	3.9
stdev	0.5	0.022	0.11	13	0.07	0.015	1.798	0.034	0.2
100:0 wx:std	13.9 ± 0.4^{a}	0.218 ± 0.010^{a}	3.97 ± 0.12^{bc}	126 ± 205^{bc}	1.37 ± 0.14^{a}	0.793 ± 0.052^{b}	18.688 ± 6.043^{c}	0.39 ± 0.19^{c}	2.8
75:25 wx:std	13.7 ± 0.3^{a}	0.213 ± 0.019^{a}	3.92 ± 0.24^{bc}	116 ± 205^{bc}	1.25 ± 0.20^{c}	0.790 ± 0.086^{a}	19.846 ± 7.956^{bc}	0.40 ± 0.22^{c}	3.1
50:50 wx:std	12.7 ± 0.5^{b}	0.212 ± 0.008^{a}	4.09 ± 0.18^{ab}	136 ± 205^{ab}	1.27 ± 0.14^{b}	0.797 ± 0.063^{ab}	20.120 ± 6.690^{bc}	0.51 ± 0.26^{bc}	4.1
25:75 wx:std	12.3 ± 0.7^{b}	0.221 ± 0.004^{a}	4.16 ± 0.18^{a}	131 ± 195^{a}	1.31 ± 0.17^{b}	0.778 ± 0.090^{ab}	24.142 ± 8.907^{ab}	0.58 ± 0.24^{b}	4.9
0:100 wx:std	10.6 ± 0.0^{c}	0.209 ± 0.008^{a}	3.85 ± 0.24^{c}	130 ± 275^{c}	1.39 ± 0.15^{a}	0.756 ± 0.091^{c}	25.732 ± 6.141^{a}	0.77 ± 0.33^{a}	6.6

MC, moisture content (n=3); EI, expansion-index (n=10); WpK, weight per kernel (n=3); LtWr, length-to-width-ratio ($n \geqslant 44$); BI, breaking-index
Means with the same superscript in the same column are significantly different ($p<0.05$, Tukey's HSD)
[1]Breaking index is defined as the relative compression depth before breaking of the extrudate occurs